A Practical Guide to FTIR Photoacoustic Spectroscopy

J.F. McClelland*, R.W. Jones, S. Luo
and L.M. Seaverson*

Center for Advanced Technology Development
and
Ames Laboratory, Iowa State University
Ames, IA 50011 USA
and
*MTEC Photoacoustics, Inc.
P.O. Box 1095, Ames, IA 50014 USA
515 292-7974 (voice), 515 292-7125 (fax)
e-mail: mtec@mtecpas.com
www.mtecpas.com

March, 1992

This is a preprint of a chapter appearing in
Practical Sampling Techniques for Infrared Analysis
edited by Dr. Patricia B. Coleman
and published by CRC Press

TABLE OF CONTENTS

I. INTRODUCTION - THE OPACITY PROBLEM AND ITS SOLUTIONS

The main sample handling problem in FTIR analysis of solid and semi-solid materials is that nearly all materials are too opaque in their normal forms for direct transmission analysis in the mid-infrared spectral region. Traditionally, the opacity problem has been remedied by reducing the optical density of samples to a suitable level by various methods of sample preparation.[1, 2, 3] This approach, however, leaves much to be desired due to the time and labor involved, the risk of sample alteration and preparation error, and the destructive nature of the process. Consequently, various other approaches have been tried to avoid or to minimize sample preparation.

One such approach is to simply avoid the opacity of the mid-infrared spectral region by using overtone and combination absorbance bands for analysis in the near-infrared spectral region where absorption coefficients are significantly lower and samples are less opaque.[4] Near-infrared spectra combined with factor analysis software are successful in many analytical applications. Unfortunately, less detailed information is extractable from near-infrared spectra due to the broad, overlapping character of near-infrared absorbance bands. Consequently, the mid-infrared, especially the fingerprint region, remains as the most information-rich spectral region for analytical purposes.

Another approach is to select one of the alternative mid-infrared sampling techniques to transmission such as specular reflectance, diffuse reflectance (DRIFTS), or attenuated total internal reflectance (ATR).[1, 2, 3] All of these are, however, limited in their applicability. Specular reflectance requires mirror-like surfaces. DRIFTS often involves particle size reduction and dilution in KBr. ATR presents problems related to the reflection element in terms of clean-up, crystal damage, and reproducible optical contact.

The most broadly-applicable mid-infrared solution to the opacity problem is photoacoustic spectroscopy (PAS).[5] Its signal generation process automatically and reproducibly isolates a layer extending beneath the sample's surface which has suitable optical density for analysis without physically altering the sample. PAS directly measures the absorbance spectrum of the layer without having to infer the desired absorbance spectrum based on a reflection or transmission measurement. This chapter will discuss PAS signal generation, instrumentation, sample handling and results obtained with various classes of samples.

II. PHOTOACOUSTIC SIGNAL GENERATION

The photoacoustic signal is generated when infrared radiation absorbed by the sample converts into heat within the sample. This heat diffuses to the sample surface and into an adjacent gas atmosphere. The thermal expansion of this gas produces the photoacoustic signal.

A. Signal Generation Model

The photoacoustic signal generation sequence is shown schematically in Figs. 1 and 2. Fig. 1 shows the infrared beam intensity incident on the sample with intensity I_0. The

beam's intensity is modulated at frequencies, f=vν, by the FTIR interferometer when the mirror moves with optical path difference velocity v resulting in a unique modulation frequency corresponding to each wavenumber ν. Alternatively, the modulation frequency can be set independent of v and ν if the FTIR interferometer has step-scan capability.[6, 7, 8]

After the infrared beam passes through the detector window and a transparent gas (typically helium), a fraction, R, is reflected at the sample's surface. The infrared beam intensity is given by $I_0(1-R)$ at a depth x=0 inside the sample and decays to a value $I_0(1-R)e^{-\alpha x}$ at depth x due to absorption of infrared radiation in the sample which has an absorption coefficient α.

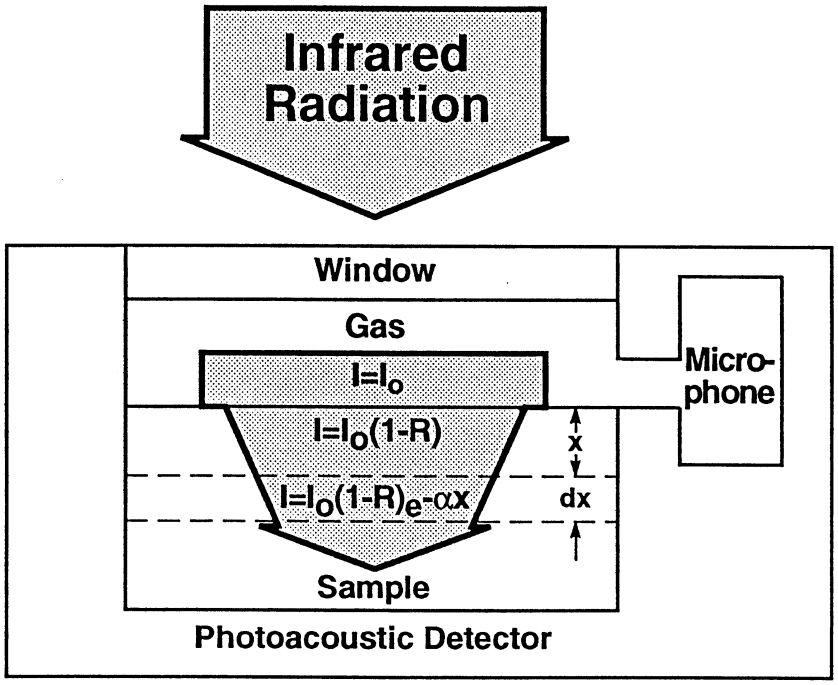

Fig. 1. Schematic of photoacoustic signal generation showing the infrared beam intensity changes upon reflection and absorption by the sample.

Each layer dx of the sample that absorbs infrared radiation experiences an oscillatory heating at frequencies f with temperature change amplitudes, ΔT, proportional to $I_0(1-R)\alpha e^{-\alpha x}dx$ as shown in Fig. 2. Each sample layer that oscillates in temperature is a source of thermal-waves.[9] In the one-dimensional energy flow schematic of Fig. 2, thermal-waves propagate from the sample's bulk to the irradiated surface and into the adjacent gas. During propagation thermal-waves decay with a coefficient $a_s=(\pi f / D)^{1/2}$ where D is the sample's thermal diffusivity.[10] Consequently, the surface temperature oscillation amplitude ΔT_S is proportional to $I_0(1-R)\alpha e^{-(\alpha+a_s)x}dx$ for a thermal-wave generated at depth x just before it crosses into the gas adjacent to the sample surface. A fraction, R_t, of the thermal-wave is reflected back into the sample at the surface resulting in a temperature oscillation amplitude in the gas ΔT_g proportional to $I_0(1-R)(1-R_t)\alpha e^{-(\alpha+a_s)x}dx$.

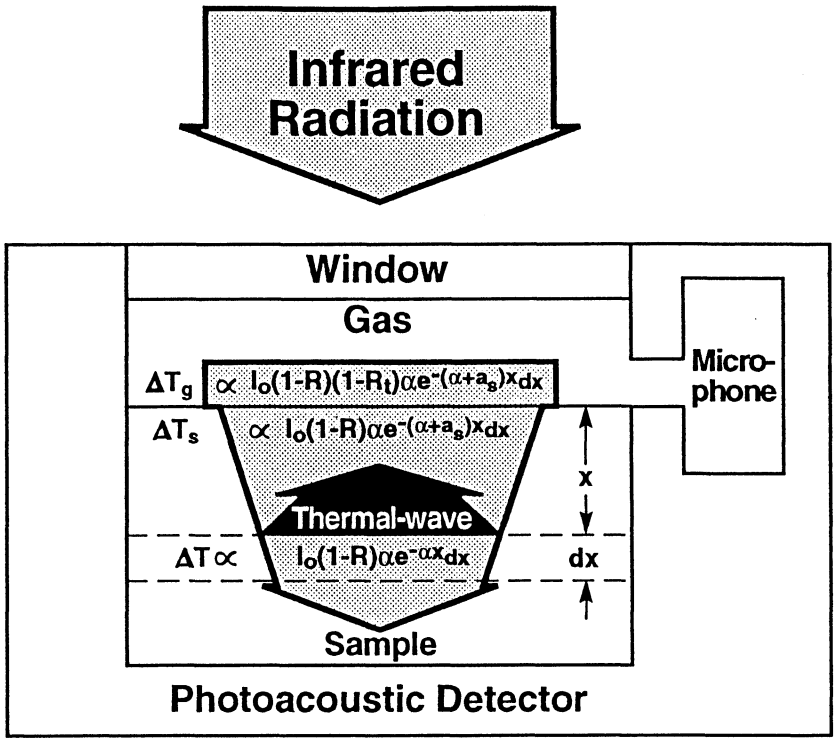

Fig. 2. Schematic of one-dimensional photoacoustic signal generation showing the temperature changes that occur in the sample and adjacent gas.

The photoacoustic signal is generated by thermal expansion of the gas caused by heat associated with the sum of all of the ΔT_g contributions. Contributions come from each of the sample layers in which energy of the infrared beam is absorbed and which is close enough to the surface so that the thermal-wave amplitude has not decayed to a vanishing contribution after crossing the sample-gas interface.

Both the infrared and thermal-wave decay coefficients, α and a_s, respectively, play a key role in photoacoustic signal generation. The term $\alpha e^{-(\alpha+a_s)x}$ in the temperature oscillation expression leads to a linear photoacoustic signal dependence on infrared absorption when $\alpha << a_s$. In this situation a layer of sample extending a distance $L=1/a_s$ beneath the surface contributes 63% ($=e^{-a_s L}$) of the signal with the other 37% coming from deeper layers of the sample. The thermal-wave decay length L is referred to as the sampling depth of a FTIR-PAS measurement.

The possibility of varying the sampling depth of FTIR-PAS measurements via the mirror velocity is apparent when L is written as $L=1/a_s = (D / \pi\nu v)^{1/2}$ where the substitution $f=\nu v$ has been made. Note also that the sampling depth increases with decreasing wavenumber by more than a factor of three across the spectrum of a sample going from 4000 cm^{-1} to 400 cm^{-1}. A constant sampling depth, $L=(D / \pi f)^{1/2}$, versus wavenumber is obtained with FTIR systems operating in the step-scan mode that allows a constant

modulation frequency to be selected and detected independent of the mirror imposed modulation.

When $\alpha << a_s$, the photoacoustic signal increases linearly with α because as α increases, more infrared absorption occurs within the layer thickness, L, which is efficient in transporting heat into the gas. The photoacoustic signal loses linearity (the onset of saturation) as the infrared absorption continues to increase and as a high fraction of the absorption occurs within the layer. At very high infrared absorption, heating occurs very close to the sample surface and the photoacoustic signal no longer increases with infrared absorption (full saturation). After full saturation some spectral features may still be observed due to spectral variations in the (1-R) term of the photoacoustic signal expression.

FTIR-PAS spectra usually contain bands with infrared absorption coefficients in the ranges both before and after the onset of saturation but spectral features due to reflectivity effects associated with full saturation are a very minor presence and often are not discernable. The onset of saturation can be moved to higher absorption by increasing modulation frequency and thereby decreasing the sampling depth. In most quantitative analyses, however, signal saturation does not present a problem due to the presence of weaker bands that are linear with concentration and the tolerance of commercial FTIR factor analysis software to nonlinearities in spectra.

B. Variation of Sampling Depth

In the analysis of samples with concentration gradients or layers it is particularly desirable to be able to vary the sampling depth. The most straight forward situation is one where: (i) the thermal diffusivity is homogeneous, (ii) the weak absorption bands (such that α values at absorbance band peaks are $<< a_s$) can be used both for monitoring the depth-varying concentration and (iii) an internal standard absorbance band is available which is associated with a species that doesn't vary with depth. Furthermore, the sample's thermal diffusivity D and the modulation frequency f must allow the sampling depth $L = (D / \pi f)^{1/2}$ to be adjusted over the range of interest by setting f via the mirror velocity or the step-scan modulator.[8, 11]

Table 1 gives sampling depths for typical values of thermal diffusivities and modulation frequencies. The thermal-wave decay coefficient, which should be larger than the analysis peak absorption coefficient value, is just the reciprocal of the sampling depth as discussed in the last section. FTIR-PAS sampling depths for polymers are typically in the micrometer to hundreds of micrometers range. This range nicely compliments ATR measurements which typically have sampling depths ranging from fractions of micrometers to micrometers.[12]

Table 1. Sampling depths in μm for typical thermal diffusivities from 0.1 to 0.0001 cm^2/s and modulation frequencies from 10^{-1} to 10^4 Hz. D is given by $k/\rho C$ where k, ρ, and C are the thermal conductivity, density and specific heat of the material, respectively.

$D(cm^2/s)$	0.1 Hz	1 Hz	10 Hz	100 Hz	1000 Hz	10000 Hz
0.1	6000	2000	600	200	60	20
0.01	2000	600	200	60	20	6
0.001	600	200	60	20	6	2
0.0001	200	60	20	6	2	0.6

Nonhomogeneous samples are more difficult to analyze when the thermal diffusivity varies significantly with depth and when the absorption coefficient is not small relative to the thermal-wave decay coefficient. Variations in the thermal diffusivity between thin layers of a material result in variations in sampling depth within the sample and in thermal-wave reflection effects[9] at layer interfaces, both of which make interpretation of results more complicated. Analyses based on stronger absorption bands also can lead to ambiguities since the sampling depth is now determined by the decay of both the infrared beam and thermal-waves within the sample. Furthermore, when the sampling depth is reduced by increasing the modulation frequency, reduction occurs in the saturation induced truncation of strong bands. This phenomenon can be incorrectly interpreted as an increase in species concentration near the surface. (See Section V.D.).

Very useful practical information can be obtained from varying the sampling depth of FTIR-PAS measurements despite the above cautionary considerations and the frequent lack of known infrared and thermal-wave absorption coefficients. Such coefficients, when available, are used to estimate sampling depth as the reciprocal of whichever absorption coefficient (infrared or thermal-wave) is larger. In practice, it is best to use spectral regions where absorption coefficients are known to be low by comparison with other spectral bands and to estimate sampling depth from the expression $L = (D/\pi f)^{1/2}$. The thermal diffusivity is given by $D=k/\rho C$ where k, ρ, and C are the thermal conductivity, density, and specific heat, respectively. These properties can usually be found in the literature for general classes of materials, if not for a specific sample.

III. INSTRUMENTATION

A. Photoacoustic Detector

FTIR photoacoustic detector accessories are currently manufactured by Bio-Rad (Cambridge, MA USA) and MTEC Photoacoustics (Ames, IA USA) for use with FTIR spectrometers. This discussion will be limited to the MTEC model 200 unit because it is available from distributors and all major FTIR companies throughout the world. Figure 3 is

a photograph of the MTEC unit which mounts directly in the sample compartment of the FTIR's optical bench.

Fig. 3. MTEC Model 200 photoacoustic detector mounted on a Nicolet sample compartment baseplate.

The spectral range of a photoacoustic detector depends only on the transparency of the sample chamber window. With suitable windows a detector can operate from the UV to the far-infrared. The most common window material is KBr (UV through mid-infrared), but quartz (UV through near-infrared), CsI (UV - 200 cm^{-1}), ZnSe (near-infrared - 560 cm^{-1}), and polyethylene (far-infrared) are also frequently used.

The maximum MTEC sample holder dimensions are 10.7 mm in diameter by 9.0 mm deep. Most analyses require a much smaller sample volume. Sample holder inserts are provided to displace unused gas volume and boost the signal level which is proportional to the reciprocal of the gas volume.

Only the central region of the MTEC sample chamber is irradiated by the infrared beam because the photoacoustic detector's mirror causes a factor of two diameter reduction in the FTIR beam focal-spot size between the normal focus in the FTIR sample compartment and the focus in the photoacoustic detector sample holder. For instance, if the FTIR normally has a 10 mm focal-spot diameter, this size is reduced to a 5 mm diameter inside the detector sample holder at the focal plane position which is approximately 1.0 mm to1.5 mm below the detector window. Consequently, the sample volume that is actually analyzed

is approximated by the focal area times the sampling depth, L, which depends on the modulation frequency.

When helium is used in the sample chamber, the modulation frequency range of the MTEC model 200 extends from below 1 Hz to nearly 10 kHz. The use of air results in a high frequency cut-off at approximately 3kHz. Measurements at higher frequencies in air are difficult due to a substantial loss in sensitivity after the detector goes through its first Helmholtz resonance.[13] This type of resonance is due to gas oscillations in the tube between the sample and microphone chambers. Acoustic resonances in the sample chamber itself do not occur because the chamber dimensions are too small when a sample is in place.

Helium purging of the sample and microphone volumes enhances sensitivity by a factor of 2 to 3, allows higher frequency operation, and removes moisture and CO_2. Moisture and CO_2 cause spectral interference as well as photoacoustic signal generation interference. The latter interference is caused by a phase difference between photoacoustic signals generated by absorption in gases or vapors versus solids. The phase shift of gas or vapor signals leads to increased noise in spectra.

Many samples such as coal evolve water vapor after being sealed in the sample chamber. In such cases, a cup of desiccant is placed in the sample holder beneath the sample cup. Magnesium perchlorate is an excellent desiccant for this purpose and typically can be used for a day of operation without renewal.

It is important to note that moisture and CO_2 bands in spectra can be due to the presence of vapor and gas in both the FTIR optical path and the photoacoustic detector. The source location can be identified by recognizing that contamination in the FTIR causes negatively pointing (transmission-like) moisture and CO_2 bands in FTIR-PAS spectra, whereas bands are positively pointing (absorbance-like) if contamination is in the detector itself. These observations should be used as a guide in purge and desiccant operations.

A final instrumental consideration is provision for normalizing spectra to account for spectral variations in the FTIR source and optics, and for any sensitivity changes that may occur from day to day due to changes in source intensity or optical alignment. Normalization is performed by computing the ratio of the sample spectrum to a carbon black spectrum. The latter spectrum is best obtained with a MTEC reference standard consisting of an absorber element with a stable carbon black coating that is permanently mounted and protected in a dedicated sample holder. Loose carbon black is not a good standard for general use because its signal intensity varies as the powder settles and it is easily spilled or blown out of the sample cup. In some instances, a glassy carbon or graphite standard is desirable (see Section V. E.).

Many FTIR data systems erroneously label the normalized PAS spectrum as a "transmittance" spectrum rather than an absorbance spectrum. The FTIR data system should be commanded to change the label to absorbance prior to processing the data because many computer processing routines will either not operate or will produce incorrect results if a spectral file carries the wrong ordinate axis designation.

B. FTIR Spectrometer[14]

The signal-to-noise ratio of FTIR-PAS measurements depends on the FTIR spectrometer's performance level as well as the detector sensitivity and noise level, and signal generation efficiency of the sample. Low FTIR mirror velocities produce low modulation frequencies and more efficient signal generation due to the slow thermal response of samples. Low modulation frequencies yield higher signal-to-noise spectra for a given acquisition time provided that the mirror velocity is held stable at low values by the FTIR's mirror servo-control system. A high infrared beam intensity is also beneficial and requires a large source aperture, high source intensity, and low f number optics. All commercial FTIR systems provide combinations of these beneficial features to an extent that good FTIR-PAS measurements can be performed assuming that the FTIR is in good operating condition.

Typical default operating parameters for FTIR-PAS measurements with a fast-scan interferometer are given in Table 2.

Table 2. Commonly used FTIR operating parameters for a fast-scan interferometer.

Mirror velocity = lowest available stable velocity (0.05, 0.1, 0.25 cm/s are typical)
Resolution = 8 or 16 cm^{-1}
Source aperture = maximum
Spectral range = 400 - 4000 cm^{-1}
Number of scans = 32 - 256

Mirror velocity is given in Table 2 as an optical path difference velocity, v, which allows the modulation frequency, f, at a given wavenumber, ν, to be calculated from the formula, $f=\nu v$. As discussed in the last section, the mirror velocity can be increased to decrease the sampling depth and vice versa. Step-scan systems allow a desired modulation frequency to be selected that is constant at all wavenumbers thus providing a constant sampling depth for values of absorbance below the onset of signal saturation.[8, 11] Resolution can also be adjusted for specific needs but should not be set higher than necessary to resolve the structure of interest because as the resolution is increased, noise will also increase for a set number of scans. The spectral range is dictated by the spectrometer's source and beam splitter provided that the photoacoustic detector window has suitable transparency. In the near-infrared, visible, and ultraviolet spectral regions, very low mirror velocity and step-scan interferometers are particularly useful in order to keep modulation frequencies from becoming too high at the high wavenumbers of these spectral regions. The signal-to-noise ratio increases proportional to the square root of the number of scans, therefore the number of scans can be adjusted to provide the signal-to-noise ratio necessary for a given application.

C. System Checks

At initial set-up the optical alignment of the photoacoustic detector to the FTIR infrared beam should be checked and adjusted if necessary. A liquid crystal infrared imager is supplied by MTEC for this purpose. The imager is placed in the sample holder and provides a clear direct image of the infrared beam's focal spot location. The detector should be aligned in the FTIR sample compartment by centering the focal spot in the sample holder. Kinematic detector mount positioners are supplied by MTEC and should be secured in place to register the detector alignment position so that future re-installation does not require alignment. Note that if the FTIR spectrometer in use has provision for automatic alignment of the interferometer, this alignment routine should be done prior to placing the photoacoustic detector in the FTIR. The spectrometer's own detector should be used because it has the correct position and active area size for the alignment procedure.

An FTIR-PAS signal-to-noise ratio performance test should yield a peak-to-peak noise of less than 0.2% at 2000 cm^{-1} for the conditions given in Table 3.

Table 3. Test parameters for measuring the FTIR-PAS system noise

Mirror velocity (OPD) = 0.1 cm/s
Resolution = 8 cm^{-1}
Source aperture = maximum
Spectral Range = 400 - 4000 cm^{-1}
Number of scans = 8
Apodization = Medium Beer-Norton
Sample = MTEC carbon black reference
Detector gas atmosphere = helium

Some FTIR systems may not allow exact duplication of these parameters and may not perform well enough to fully meet this noise specification. Others will exceed this specification. The adjustments that will most likely improve FTIR-PAS system performance (when necessary) are alignment of the FTIR beam splitter, and tune-up of the FTIR's mirror velocity stabilizing servo-loop at low velocities.

The reproducibility of helium purging can be tested by reloading and purging the carbon black reference several times and comparing the reproducibility of spectra. Purge times of 10 seconds before and after sealing the sample cup at a flow rate of 10 cc/sec of helium are adequate for most applications where the sample has a low moisture level. The reproducibility of sample loading can also be checked by reloading and again comparing the reproducibility of spectra.

IV. SAMPLE HANDLING

A. General Considerations

The only sample preparation necessary with FTIR-PAS measurements is to have a sample size smaller than 10 mm in diameter in order to fit into the sample holder. The thickness should not exceed 6 mm. Any sample geometry can be directly analyzed including disks, slabs, chips, chunks, pellets, powders, fibers, films, and sheets. Semi-solids and liquids can also be analyzed. Larger samples are cut or abraded to suitable dimensions, typically using a razor blade, scissors, hacksaw, cork borer (#6), or a file or abrasive. Figure 4 shows a typical sample ready for analysis.

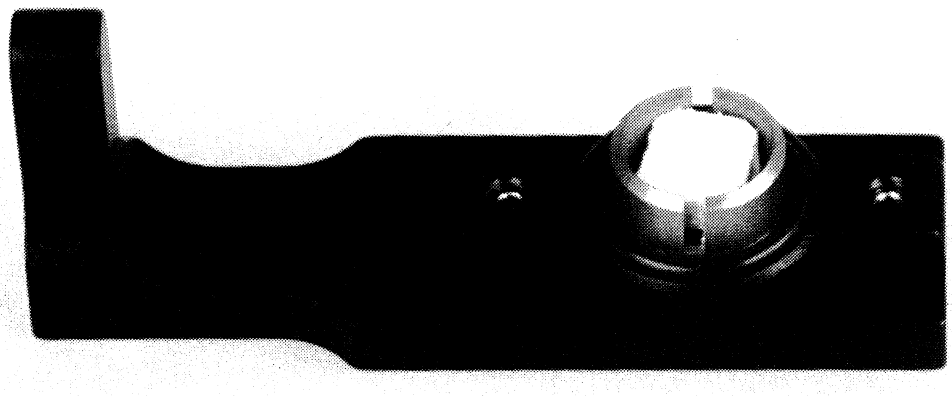

Fig. 4. Sample holder with a polymer chunk sample ready to be inserted into the photoacoustic detector.

B. Sample Loading

A MTEC sample holder is shown in Fig. 5 with large and small stainless steel sample cups and brass spacers. The latter are used to minimize the gas volume and thereby increase the photoacoustic signal. A small cup is shown in Fig. 6 placed in the sample holder. A funnel for loading powdered samples and other components for handling samples are shown in the figure also. The sample should be approximately one millimeter below the rim of the sample holder in order to allow a layer of gas between the sample and the detector window for photoacoustic signal generation in the gas. If very high or low modulation frequencies are used, an approximate distance that the sample should be below the cup rim can be calculated from the formula $(D/\pi f)^{1/2}$ where D = 1.51 cm^2/s for helium and D = 0.187 cm/s for air. The value used for f, when a rapid scan FTIR spectrometer is used, should be calculated from $f = \nu v$ where ν is the lowest wavenumber value in the spectrum.

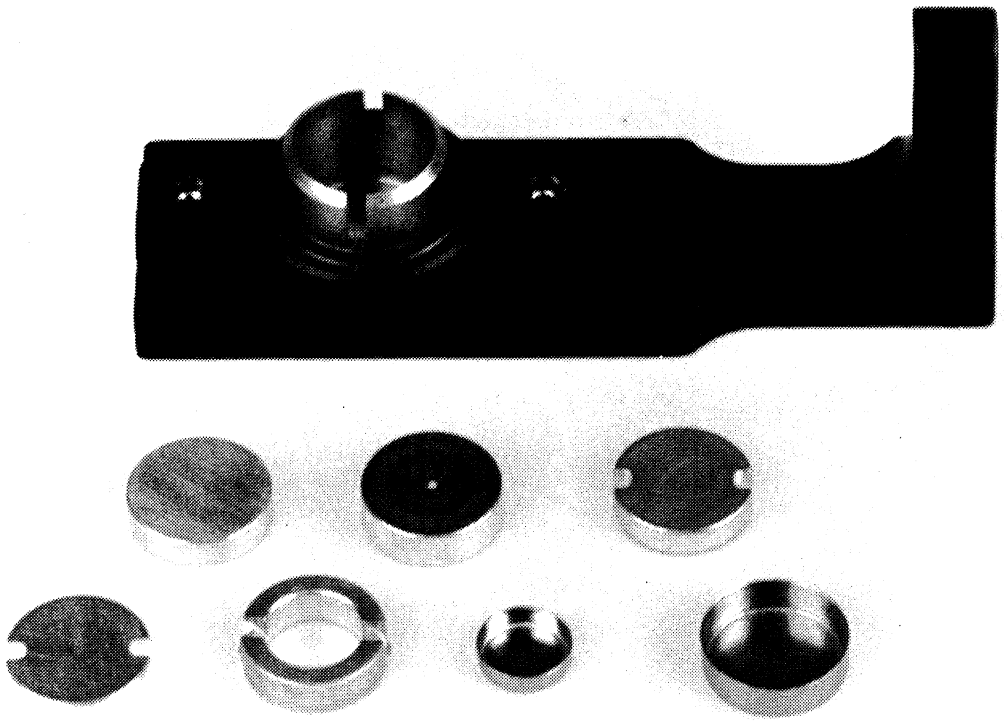

Fig. 5. MTEC sample holder, with brass inserts, and small and large stainless steel cups.

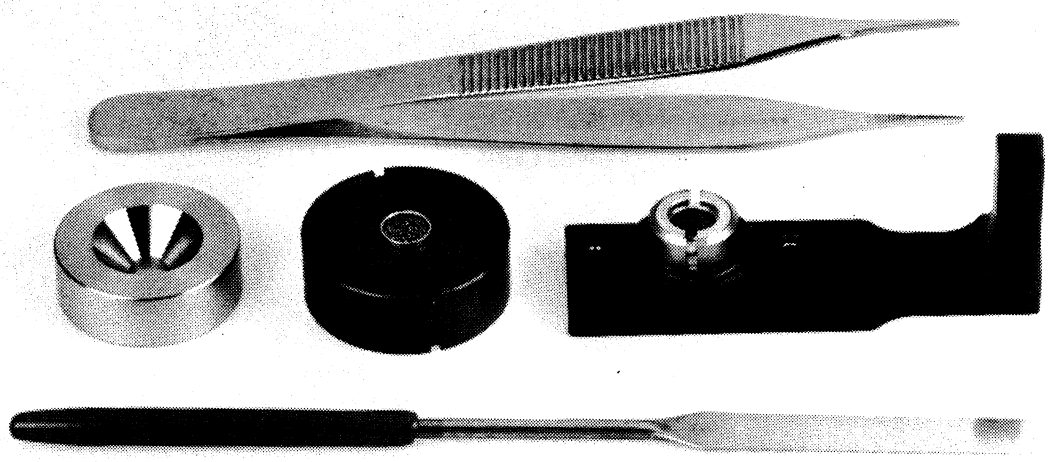

Fig. 6. Sample handling tools including sample holder loaded with small stainless steel cup, fixture and funnel for loading cups, and cup-handling tweezers and spatula.

Many samples have moisture contamination which will cause the presence of water vapor in the detector's sample chamber and the appearance of water vapor absorbance bands in spectra. A desiccant for water vapor reduction can be put into a large stainless steel cup as shown in Fig. 7 which is placed in the sample holder underneath the sample cup. Fig. 8 shows a large cup with polymer pellets which is placed above the desiccant cup. As mentioned in Section III A, magnesium perchlorate is a very effective desiccant. Water vapor can be eliminated with the combination of purging the detector with dry helium, allowing adequate time for the desiccant to work, and minimizing the amount of sample in the cup. Use only enough material to cover the bottom of a small cup if water vapor is a problem. When not in use, desiccant should never by left in cups open to the room's atmosphere because moisture from the room will collect in the desiccant and form a corrosive liquid.

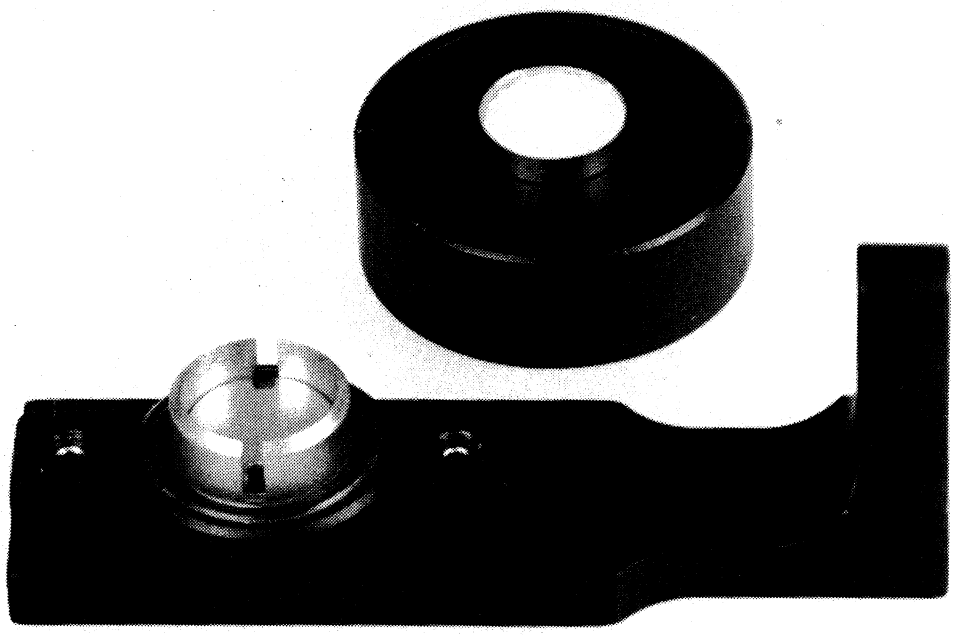

Fig. 7. Background: Large stainless steel cup loaded with desiccant resting on a cup fixture. Foreground: Desiccant cup has been placed underneath a slotted brass spacer insert in the sample holder. Sample cups are placed on the spacer. See Fig. 8.

Fig. 8 Polymer pellets in sample cup placed above desiccant cup.

V. FTIR-PAS METHODS FOR SPECIFIC ANALYSES

This section provides detailed information on how to measure spectra of important classes of samples and how to process and interpret photoacoustic spectra. All of the spectra were measured at a resolution of 8 cm^{-1}, maximum source aperture, and with a helium gas atmosphere in the detector. The spectra have been normalized by computing a ratio of the sample spectrum to the spectrum of a MTEC carbon black standard unless otherwise stated.

A. Qualitative Analysis of Macrosamples

1. Polymer identification by computer search

FTIR-PAS allows spectra of polymers in powder, pellet, sheet, and chunk form to be directly measured and searched against standard commercial spectral libraries. Figs. 4 and 8 show a chunk and pellets, respectively, that have been placed in the sample holder for analysis. Figs. 9-12 show commercial library spectra[15] and photoacoustic spectra of four common polymers. The photoacoustic spectra have been converted to transmittance to be compatible with the Perkin-Elmer commercial SEARCH™ program. Because different polymer specimens were used when the library and photoacoustic spectra were measured, there are some variations between them. The degree of band saturation at low values of transmission vary from spectrum to spectrum but is generally slightly more pronounced in the photoacoustic spectra since the library samples were in the form of thin films.

The photoacoustic spectra were measured at FTIR OPD mirror velocities from 0.1 cm/s to 0.5 cm/s. A wider velocity range should also be suitable. The spectra were searched against the Perkin-Elmer SEARCH™ library using the following procedure:

1. After the ratio of sample spectrum to carbon black spectrum is calculated, most FTIR data systems erroneously label the ordinate of the resulting spectrum as "transmittance". Scale this spectrum so that its maximum and minimum values are around 90% and 5% transmission, respectively.
2. Command the computer to relabel the ordinate in absorbance units.
3. Convert the spectrum to transmission via the FTIR software.
4. If necessary, rescale the spectrum so that the maximum and minimum are around 90% and 5% transmission, respectively.
5. Set the search threshold value at 5%.
6. Activate the search which should be based on peak positions only.

The success of this procedure was evident by higher search rankings that the Perkin-Elmer SEARCH™ software assigned to searches of the photoacoustic spectra than to searches of the library spectra shown in Figs. 9 through 12.

Procedures similar to the one above should be used with other FTIR systems. A suite of known polymer samples should be used to provide a basis for any refinements that might be necessary for a particular FTIR software package.

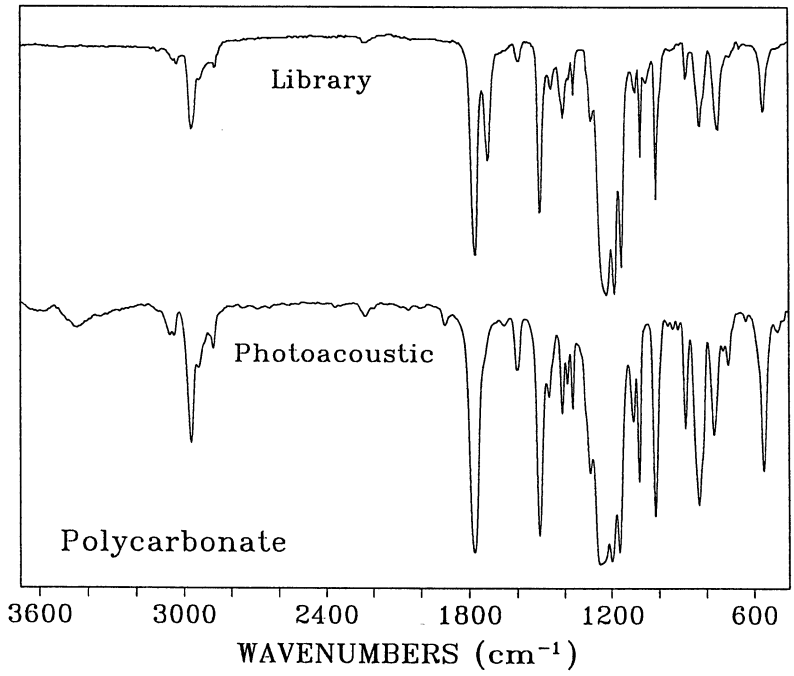

Fig. 9. Library and photoacoustic spectra of polycarbonate.

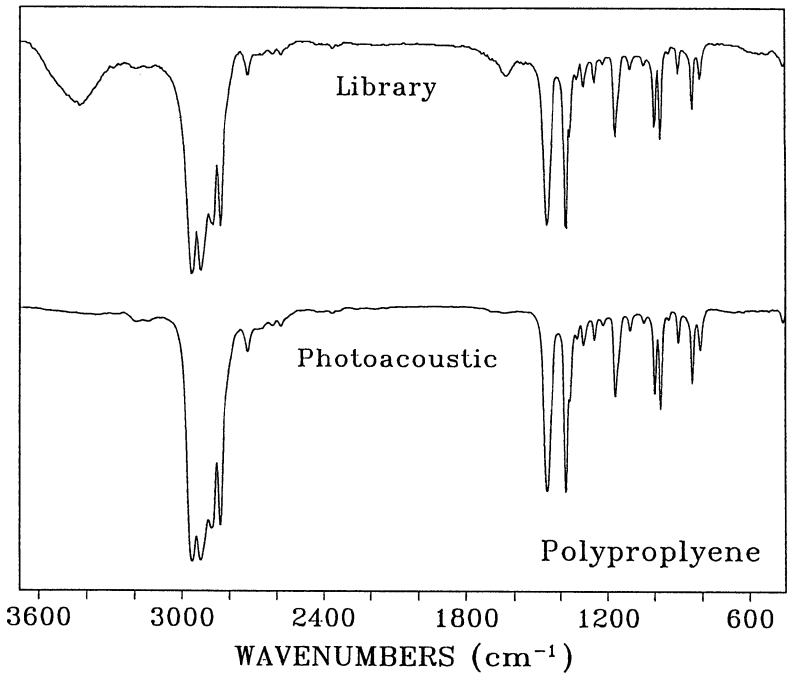

Fig. 10. Library and photoacoustic spectra of polypropylene.

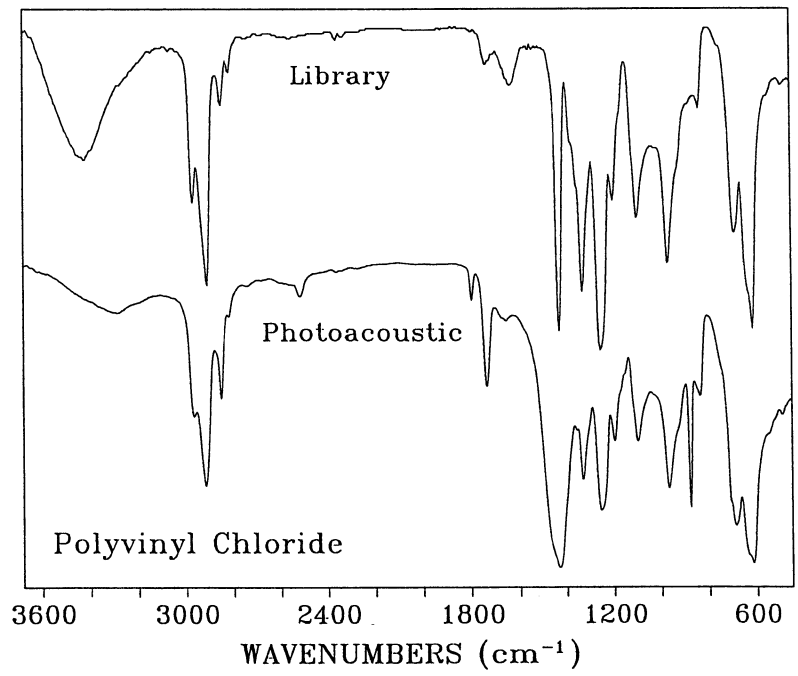

Fig. 11. Library and photoacoustic spectra of polyvinyl chloride.

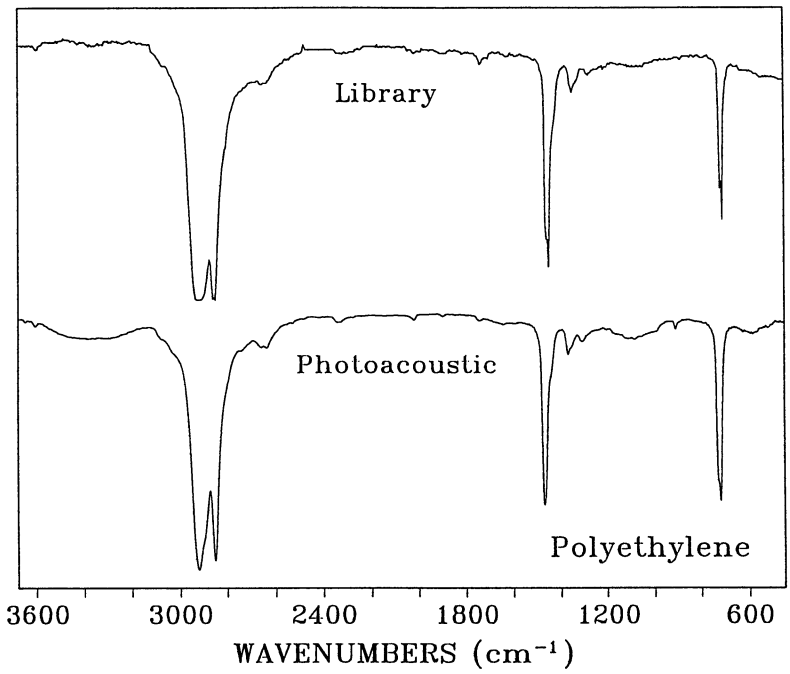

Fig. 12. Library and photoacoustic spectra of polyethylene.

2. Adhesive spectrum by spectral subtraction

Spectral subtraction is a very useful procedure in qualitative analyses in order to separate one component from a background spectrum. If the sample is a two-layer system such as a coating on a substrate, spectra can be measured separately of the coated and bare sides followed by a spectral subtraction to isolate the coating spectrum. The FTIR mirror velocity should be set high enough to perform shallow sampling in order to increase the intensity of coating bands in the spectra. Fig. 13 shows spectra of an adhesive-coated polyethylene film material, the bare polyethylene and the adhesive spectra obtained by spectral subtraction. This spectral subtraction approach should be used when it is not possible to isolate the coating sufficiently by increasing mirror velocity alone.

The upper adhesive spectrum of Fig. 13 was obtained by a straight spectral subtraction of the two top spectra without scaling one relative to the other. This results in small negative pointing features denoted by stars in the upper adhesive spectrum due to a weakening of the polyethylene substrate photoacoustic signal by the adhesive coating. The weakening is a consequence of the decay of thermal-waves as they cross the coating before reaching the gas. This reduces the amplitude of the polyethylene bands in the top spectrum of the coated-side relative to the bare-side spectrum.

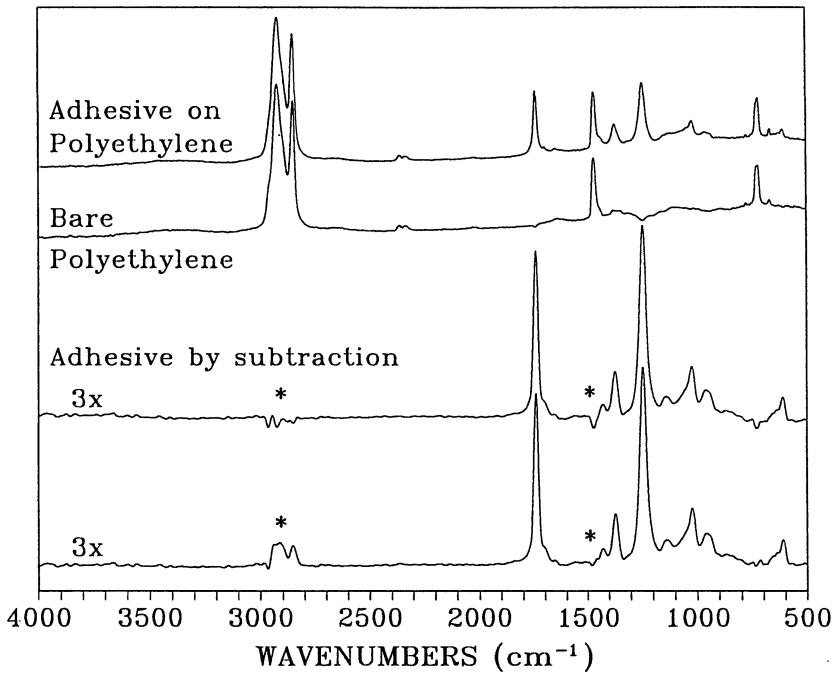

Fig. 13. Spectra of an adhesive-coated polyethylene material, of bare polyethylene and of the adhesive obtained by spectral subtraction. The upper subtraction spectrum was obtained by a direct subtraction and the lower by interactive subtraction to remove the negative features at the starred locations.

The lower adhesive spectrum of Fig. 13 was obtained by interactive spectral subtraction with a small scale change between the two top spectra to correct for the quenching phenomenon prior to subtraction. The correction to the starred features of the lower adhesive spectrum is not exact, probably due to a phase shift associated with the transit time of the thermal-wave crossing the coating. These small remaining artifacts have a derivative-like character associated with slight band shifts. Such small spectral distortions, however, do not prevent a spectral search from predicting the primary adhesive component to be vinyl acetate.

Interactive subtractions may also be necessary when non-layered samples of varying composition are analyzed if their thermal properties vary significantly with composition. When interactive FTIR-PAS spectral subtraction is used, it is necessary with many FTIR data systems to change the data file ordinate label from transmittance to absorbance units prior to performing the interactive subtraction.

B. Qualitative Analysis of Microsamples

1. Single textile fibers

FTIR-PAS offers some unique advantages for microsample analysis over FTIR microscopy:

1. No pressing of samples is required to reduce optical density. This avoids the destruction of evidence in forensic analyses, and questions of reproducibility and sample alteration posed by the pressing operation. The nondestructive character of FTIR-PAS allows analyses confirmation by other techniques such as optical or electron microscopy.

2. The delicate optical alignment and aperturing of FTIR microscopy is avoided because FTIR-PAS microsampling can be done with a beam focal spot size that is much larger than the sample since only the portion of the beam that impinges on the sample generates a photoacoustic signal.

3. The spectral range of measurements is not limited by the cut-off of narrow band MCT detectors commonly used in FTIR microscopy. The extended spectral range of FTIR-PAS microsample spectra allows better spectral differentiation between difficult samples such as nylons.

4. FTIR-PAS spectra of fibers have more easily discernable detail because normally weak but definitive bands are more prominent due to truncation of strong bands by photoacoustic signal saturation and to enhanced structure at low wavenumbers from more efficient signal generation at low frequencies.

A key consideration in FTIR-PAS microsample analyses is mounting the sample so that it is surrounded by helium gas for efficient signal generation. Fig. 14 shows devices supplied by MTEC that are used to mount single fibers and particles for FTIR-PAS analyses. Tweezers are used to mount fibers in spring loaded split rings before placement in the sample cup. In front of the sample holder is a fixture which holds the ring with either a white or black centering pin to provide a contrasting background during mounting of fibers. In the procedure, fibers are either attached by pressure sensitive adhesive to the arms of the device shown in Fig. 14 in front of the ring fixture, or fibers can be manipulated with tweezers during mounting. This operation can be done using an illuminated bench magnifier with a contrasting background. A microscope is not required. In Fig. 15 a black thread depicts a fiber being mounted and placed in the sample holder over a covered desiccant cup. The desiccant cup is shown in Fig. 14 on the left side of the ring fixture. A magnesium perchlorate desiccant and a dry helium gas atmosphere are required in microsampling because otherwise the water vapor signal, which is out-of-phase with the sample signal, can dominate the sample signal and seriously degrade the spectrum.

Fig. 14. Components of the MTEC microsampling system for particles and fibers as described in the text.

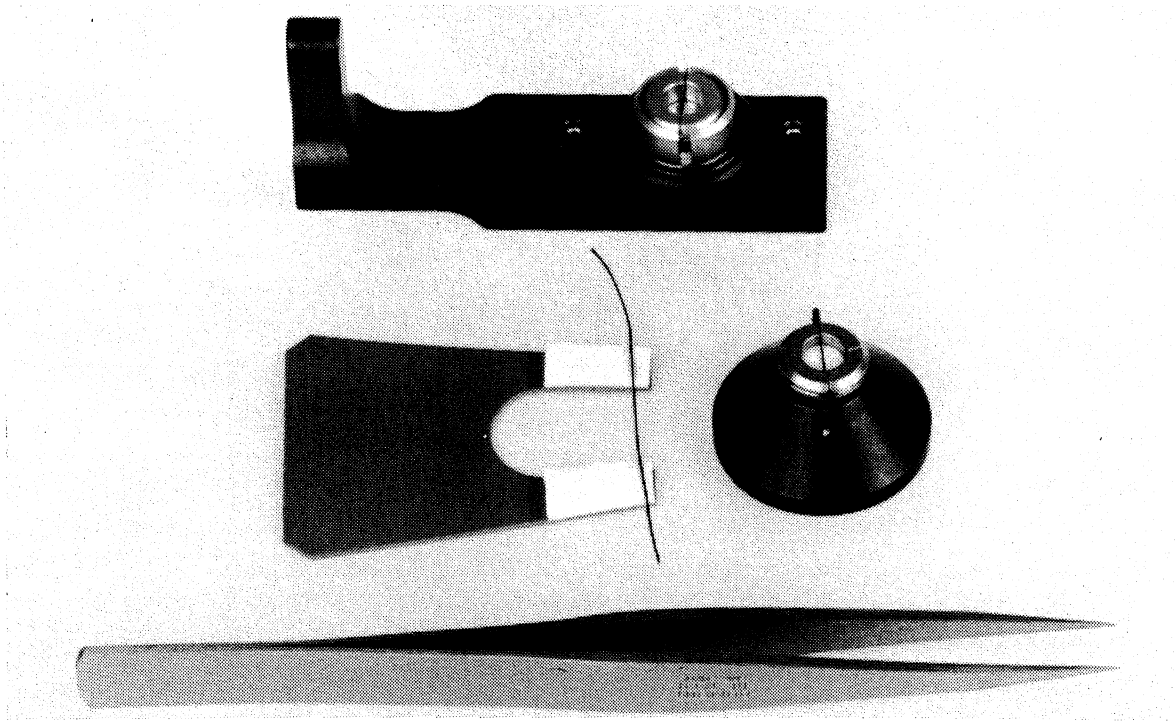

Fig. 15. Black thread depicting a fiber being mounted and placed in the sample holder over a covered desiccant cup.

Fig. 16 shows an alternative fiber mounting method that uses rings with an adhesive to attach fibers. In this approach the fiber is first stretched between two pieces of double stick tape that are attached to a light or dark release paper to give a contrasting background for the fiber. A ring with an outer ring of double stick tape is centered over the fiber and pressed against it. The ring sticks to the fiber but not to the release paper. The fiber is then cut at the outer diameter of the ring and the ring is placed in the sample holder with a second ring on top of it to mask the adhesive from the infrared beam. This second ring thereby prevents generation of a photoacoustic signal from the adhesive.

The brass rings used for this mounting technique are 1.5 mm thick, and have outer and inner diameters of 10.6 mm and 5.0 mm, respectively. The adhesive used is 3M double stick tape which is cut into rings by first applying it to a release paper of the type commonly used to cover adhesive surfaces of labels. Cork borers (sizes 4 and 6) are used to cut the adhesive rings which are then transferred to the brass rings. The adhesive ring's inner diameter is larger than the brass ring's inner diameter which helps to prevent the infrared beam from impinging on the adhesive and generating an adhesive spectrum. Adhesive coated rings can be reused a number of times if care is taken to remove the previously mounted fiber.

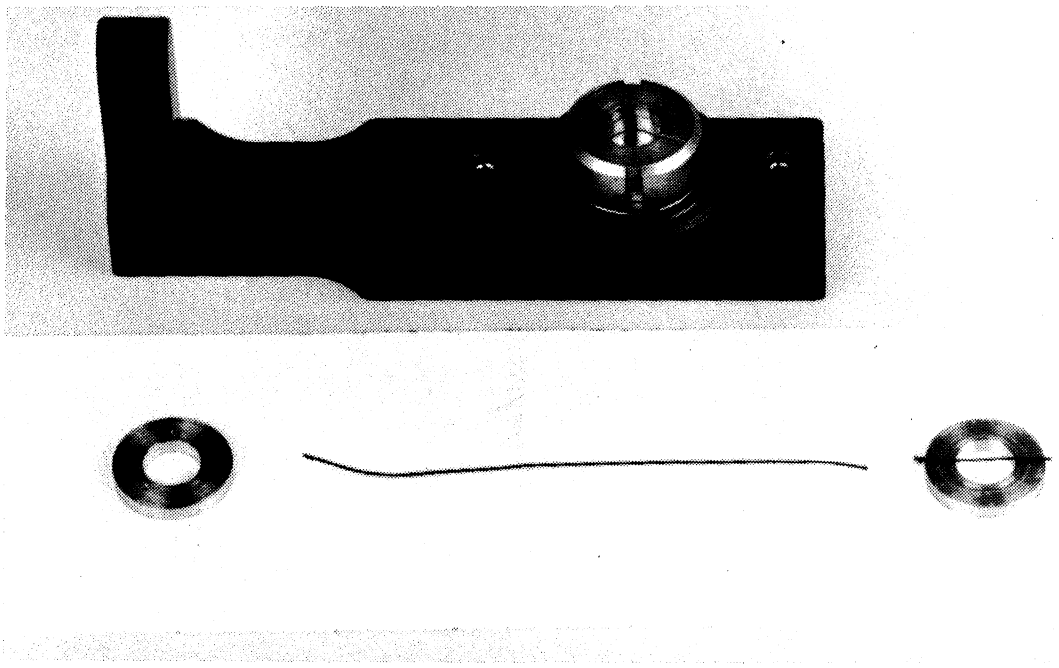

Fig. 16. Fiber mounting using a ring with an adhesive to secure the fiber.

The best results on single fibers are achieved with low FTIR mirror velocities which provide a relatively stronger fiber versus vapor signal. Fibers as small in diameter as 10 micrometers are run routinely. Smaller diameter fibers should also be practical for FTIR-PAS analysis but are not commonly presented for analysis.

FTIR-PAS spectra of the common types of nylon fibers appear in Fig. 17. These fibers are specimens from a fiber library assembled by the US Federal Bureau of Investigation (FBI) forensic science program.[16] The strong absorbance bands of the FTIR-PAS spectra are truncated due to photoacoustic signal saturation but this does not detract from their value for qualitative analyses. Spectra of nylon fibers which are not in the FBI collection have been identified successfully using a FTIR-PAS spectral library of the FBI fibers for computer searching. The fibers used to produce the two top spectra of Fig. 18 are not in the FBI collection but were identified as nylon 6,6 when computer searched against the library. The lower spectrum of Fig. 18 is the nylon 6,6 spectrum from the library. The peak positions of the two upper spectra are well matched to those of the lower library spectrum. The two upper spectra also show that variations are observed in relative peak intensities and shapes due to differences in fiber diameter and cross-sectional geometry. These variations provide additional information beyond just polymer type and could be useful in establishing that two fibers in a forensic investigation are from a common source.

The FBI collection consists of approximately 50 fibers and includes all of the common types of polymers. Over 20 FTIR-PAS spectra have been searched successfully against an FTIR-PAS spectral library of the FBI fibers without any false identifications.

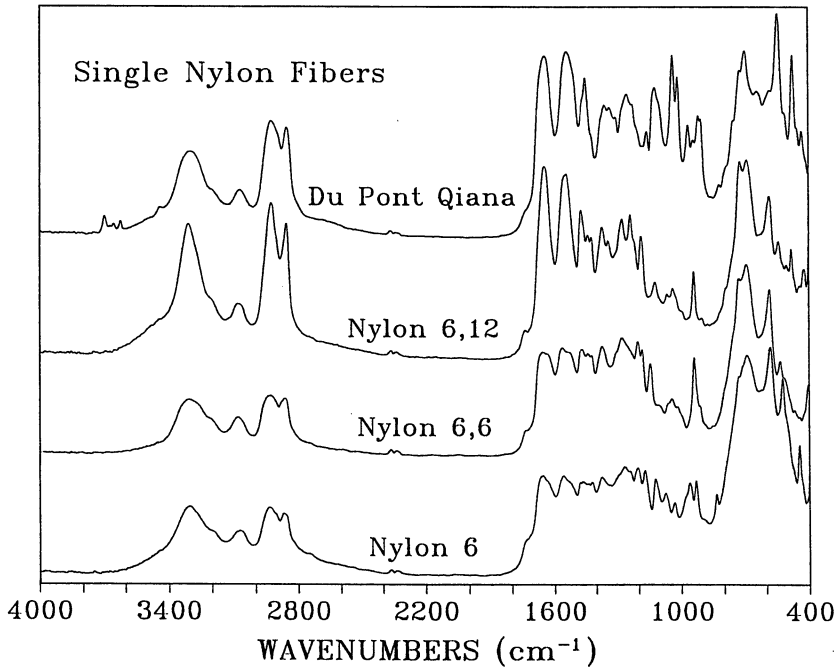

Fig. 17. FTIR-PAS spectra of four common types of nylon single fibers.

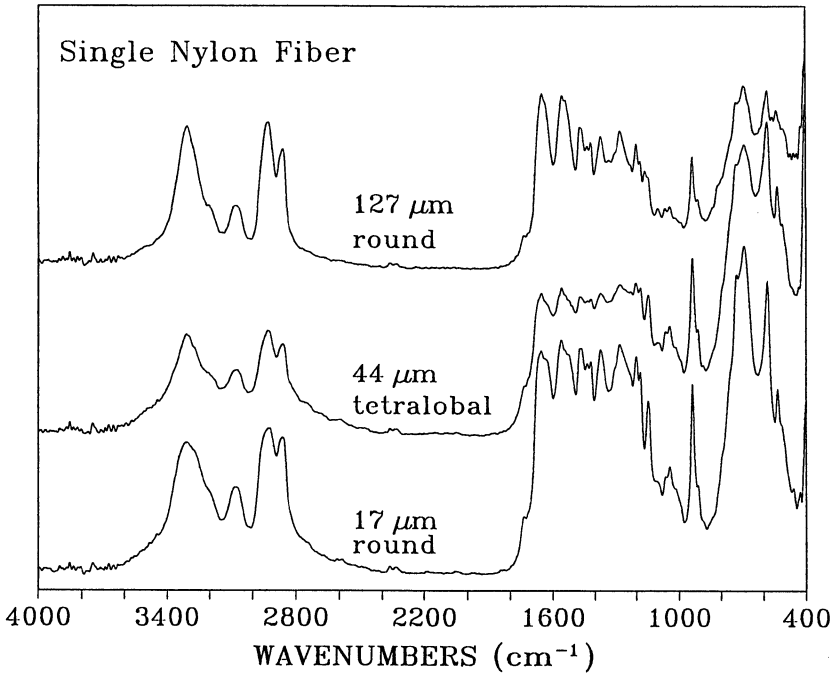

Fig. 18. FTIR-PAS spectra of single nylon 6,6 fibers with different cross-sectional geometries and fiber diameters.

2. Single coal particles

Microparticles are supported on very fine tungsten needles for FTIR-PAS analysis. Manipulation of microparticles by tungsten needles is a common practice in optical microscopy[17] and is often done by hand under a microscope by experienced microscopists. Particles usually attach to the needle tip by electrostatic attraction. In some instances when humidity is high, particles are best attached using a speck of electrically conducting colloidal graphite glue that can be obtained from distributors of microscopy supplies. The glue is made to flow using isopropanol, then the particle is rapidly touched before the glue dries. This latter method of attachment allows for both FTIR and SEM analysis of microsamples after mounting.

Microparticles are manipulated and mounted for FTIR-PAS analysis using items shown in the right foreground and background of Fig. 14. The sample holder in the photograph contains a desiccant holder, tungsten needle socket, and polished conical insert that are used in FTIR-PAS particle analysis. In the right foreground and background are a tungsten needle storage holder and a micromanipulator for the needles, respectively. The micromanipulator attaches to a laboratory microscope as shown in Fig. 19 and allows precise control of the needle point.

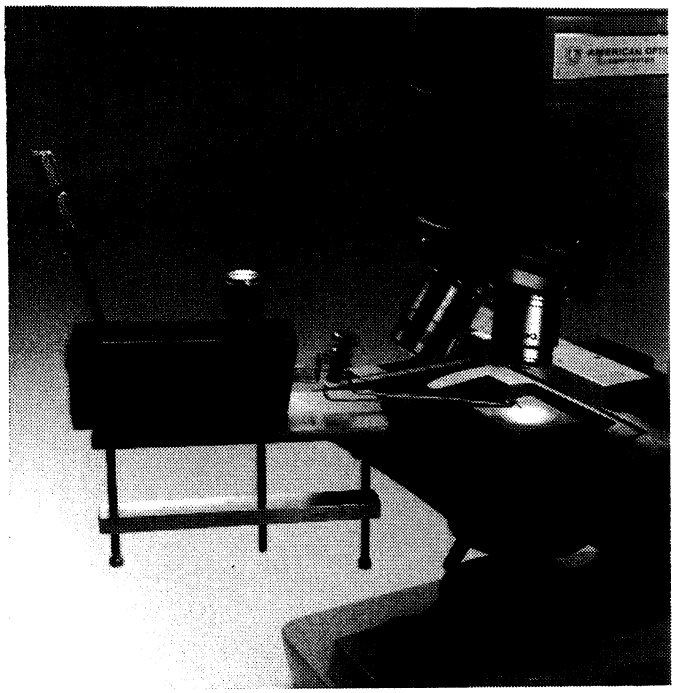

Fig. 19. Micromanipulator attached to a laboratory microscope. The manipulator allows precise control of the tungsten needle which is used to pick up particles for analysis.

The best FTIR-PAS spectra of microparticles are obtained with low mirror velocities, a helium gas atmosphere, and adequate time for the desiccant to work. It is possible to measure spectra of single particles as small as 25 micrometers in diameter with the standard 2x reduction mirror of MTEC photoacoustic detectors at an OPD FTIR mirror velocity of 0.05 cm/s. FTIR-PAS analysis of smaller particles should be possible with higher concentration of the beam intensity on the sample and lower mirror velocity.

Spectra of three single coal particles are plotted in Fig. 20 with a macrosample spectrum of the same coal at the top of the figure. The coal particle size is between 125 and 150 micrometers. The particle spectra show that there are a number of compositional differences in coal particles in this size range related to mineral, hydroxyl, and aromatic/aliphatic concentrations.

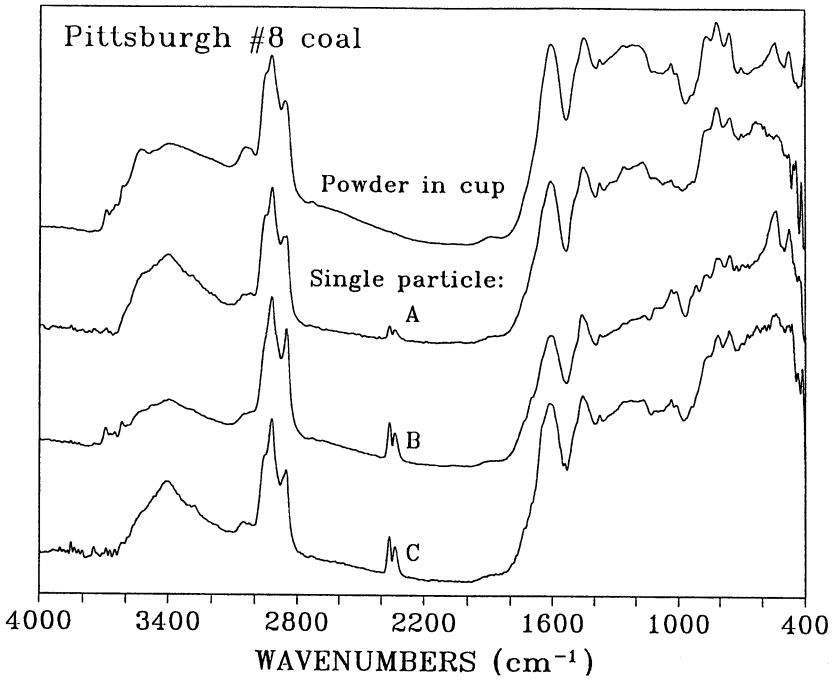

Fig. 20. FTIR-PAS spectra of coal in powder (upper) and single particle form (A, B, and C). Variations in the mineral content of the particles are indicated by bands in the 400-1000 cm^{-1} and 3600-3700 cm^{-1} regions.

C. Quantitative Analyses

The application of factor analysis for processing FTIR-PAS spectra enables quantitative analyses to be readily performed with standard error of prediction (SEP)[18, 19] values below 1% in spite of the truncation of strong absorbance bands that occurs due to photoacoustic signal saturation. Both principal components regression (PCR)[20] and partial least squares (PLS)[20] factor analysis routines tolerate nonlinearities in spectra well and allow concentrations of multicomponent systems to be determined as well as other physical and chemical properties of materials. The quality of the analysis of the FTIR-PAS technique is sensitive to the same considerations as other FTIR sampling methods. These items should be considered when a new quantitative method is being developed for a specific application.

1. The number of learning set samples used and the differences between their physical or chemical property values and those of the unknowns.
2. The provision for several learning set samples with physical or chemical property values above and below those of the unknowns.
3. The accuracy of the learning set.
4. The spectral range or ranges used in the factor analysis.
5. The spectral resolution of spectra.
6. The signal-to-noise ratio of spectra.
7. The system response stability over time and the reproducibility from sample to sample.

The first six considerations are very important to the accuracy of quantitation but are not specific to the sampling method used and will not be discussed in detail here. The last consideration depends on the FTIR, the sampling accessory, the samples, and the background

spectrum. The following conditions must remain constant or be accounted for in quantitative FTIR-PAS analyses:

1. FTIR mirror velocity
2. FTIR and PAS detector amplifier gain settings
3. PAS detector optical alignment
4. FTIR source intensity
5. FTIR interferometer alignment
6. Helium gas concentration in the PAS detector
7. Sample volume
8. Sample morphology
9. Sample matrix
10. Microphone sensitivity
11. Carbon black standard response

The FTIR mirror velocity must be set at the same value when spectra of the calibration standards (learning set) and of unknowns are acquired. If the mirror velocity setting is not maintained, changes in the PAS sampling depth will occur which are analogous to changing sample thickness or concentration in transmission spectroscopy.

All amplifier gain settings should be at the same values when sample spectra are acquired in order to have consistent measurement conditions.

Good quantitative analyses also require that the detector positioning in the FTIR is reproducible when the accessory is put in and taken out of the FTIR and that its position remains fixed when the accessory is installed. Properly designed kinematic mount and baseplate registration accomplish these requirements.

Scale variations are caused in FTIR-PAS spectra if changes occur in source intensity, interferometer alignment, helium concentration; sample volume, morphology, and matrix; and microphone sensitivity and carbon black response. In some instances, if proper care is taken, these changes can be held small enough to yield satisfactory quantitative analyses. But in most instances, adding a standardization procedure that addresses all of these potential changes is the best way to insure that quantitative results will have the degree of reproducibility necessary for a particular application.

FTIR-PAS spectra are usually best standardized by one of two methods. The first is applicable to situations where the spectral changes over the full analyte range are small relative to the whole spectrum. In this case the spectra can be scaled so that the area under the whole spectrum from 400-4000 cm^{-1} is held constant.

The second method exploits the fact that highly saturated bands in FTIR-PAS spectra vary much slower with changes in analyte concentration than do unsaturated bands. Consequently, FTIR-PAS spectra can be standardized by scaling spectra so that a particular intense band's height or area remains constant.

Both of the standardization methods appear to work well with factor analysis routines. Standardization methods should be tested and adjusted, if necessary, after a cross-correlation test of the calibration spectra. This test involves using each calibration standard, in turn, as an unknown and the others as the learning set, and then calculating the standard error of prediction.[18, 19]

In the following two examples, quantitative analyses are performed in one case with and in the other without standardization of spectra.

1. Vinyl acetate concentration in polyethylene copolymer pellets

Vinyl acetate concentrations in pellets of varying sizes are determined by FTIR-PAS and a PLS factor analysis routine (Spectra-Calc, Galactic Industries Corp., Salem, NH, USA) without sample preparation. The direct analysis of pellets is complicated by variations in sample volume and morphology. This variability and the other potential changes listed above are accounted for by using the area under the C-H band (2750 - 3120 cm^{-1}) for standardization of spectra. The analysis conditions are given in Table 4. A cross-correlation analysis of the standards set resulted in a SEP value of 0.55% (mass). The reproducibility of the PLS analysis was tested by twice running spectra on pellets of three concentrations. The second run involved reloading the same pellets in the sample cup followed by the purge and seal operation, and spectrum acquisition. The average values of the vinyl acetate concentrations were 5.89%, 9.49%, and 16.27% and the differences between the two analysis values for each concentration were 0.12%, 0.21%, and 0.00%, respectively. The manufacturer's stated concentrations for the samples were 5.84%, 9.36%, and 14.90%. All of the data are consistent with the cross-correlation analysis SEP except for the highest concentration value reported by the manufacturer.

Figure 21 shows typical FTIR-PAS spectra of two vinyl acetate-polyethylene copolymer samples that were in the learning set. The cross-correlation analysis results are plotted in Fig. 22.

2. Ash concentration in coal

In industry, coal is cleaned by various processes in order to reduce the concentration of ash which causes boiler fouling and environmental problems. The froth flotation cleaning process produces float material with reduced ash concentration and a sink material with high ash content. FTIR-PAS can be used to rapidly check the ash concentration in a coal cleaning operation using standards that are synthesized from float and sink material. The analysis conditions are given in Table 4. The coal samples were in fine powder form and were formulated to have different ash concentrations by mixing calculated weights of float and sink material. Portions of the mixtures were measured out for FTIR-PAS analysis by volume simply by filling small stainless steel sample cups as shown in Fig. 5 and sliding a spatula across the cup rim to remove excess powder. Fig. 23 shows two typical spectra of the float (6% ash) and sink (31.6% ash) material that were used in the analyses. The results of the cross-correlation analysis are plotted in Fig. 24. A SEP of 0.44% (mass) was obtained.

Table 4. Analysis conditions for determinations of vinyl acetate in polyethylene copolymers and ash in coal. Standard errors of prediction (SEP) are given for cross-correlations of the standards set.

Condition	Vinyl Acetate	Ash
number of scans	128	64
OPD mirror velocity (cm/s)	0.10	0.05
resolution (cm^{-1})	8	8
number of standards	13	11
concentration range	8.81 - 51 %	6.0 - 31.6 %
type of standards	pellets of different sizes	-200 mesh powder
method of analyzing standards	titration	ASTM ash analysis
type of factor analysis	PLS	PCR
spectral ranges of factor analysis	578-1596 cm^{-1}, 1630-1900cm^{-1}, 2479-3150 cm^{-1}	720 - 1818 cm^{-1}
spectrum standardization	area of CH band 2750 - 3120	none
number of data sets averaged	3	1
SEP	0.55% (mass)	0.44% (mass)

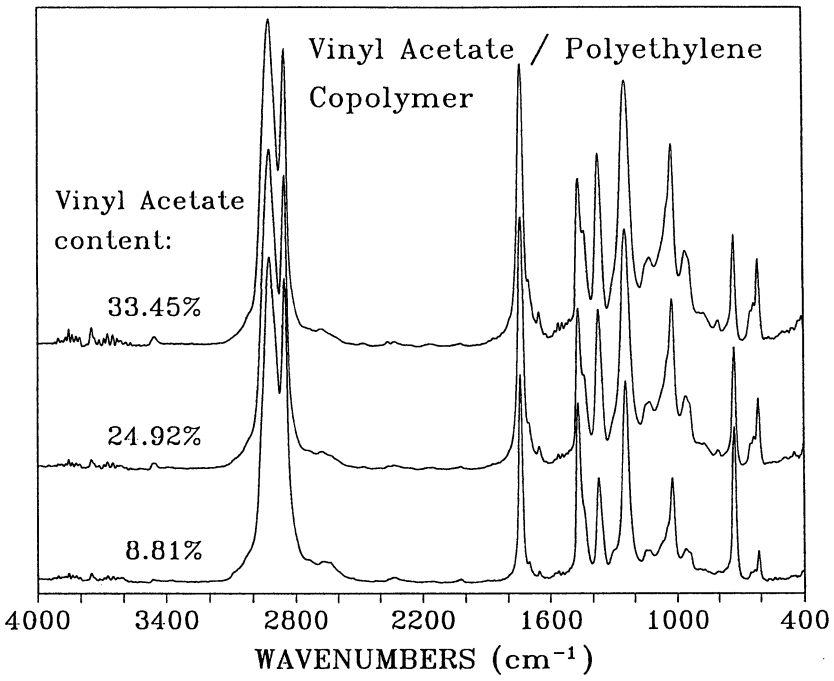

Fig. 21. FTIR-PAS spectra of three compositions of vinyl acetate/polyethylene copolymers.

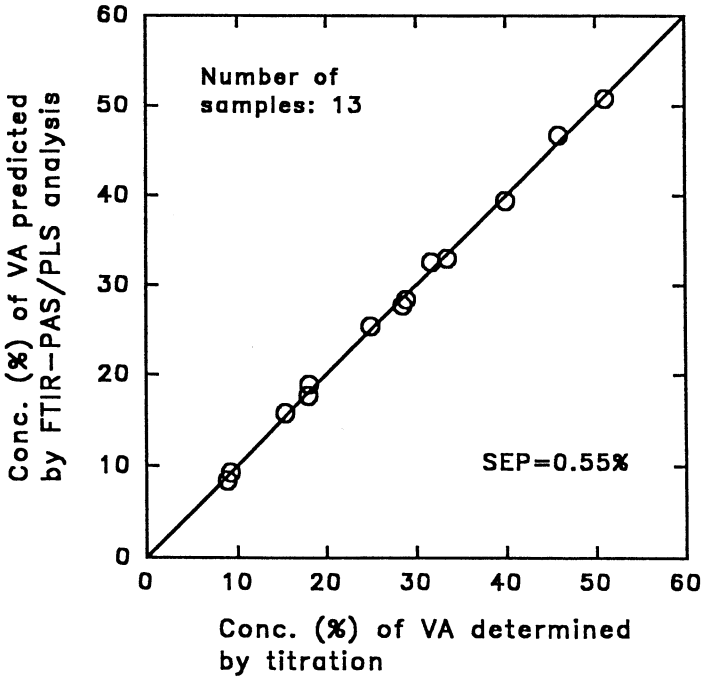

Fig. 22. Cross-correlation plot of vinyl acetate concentration determined by titration against predicted concentration by FTIR-PAS/PLS analysis for pellet vinyl acetate/polyethlene copolymer samples.

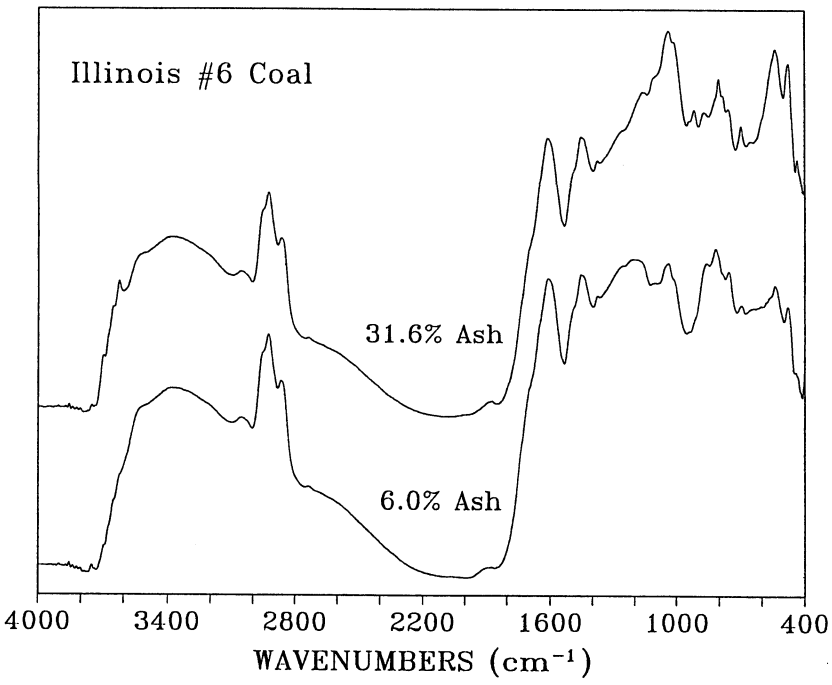

Fig. 23. FTIR-PAS spectra of two typical samples of float and sink material from cleaning Illinois #6 coal.

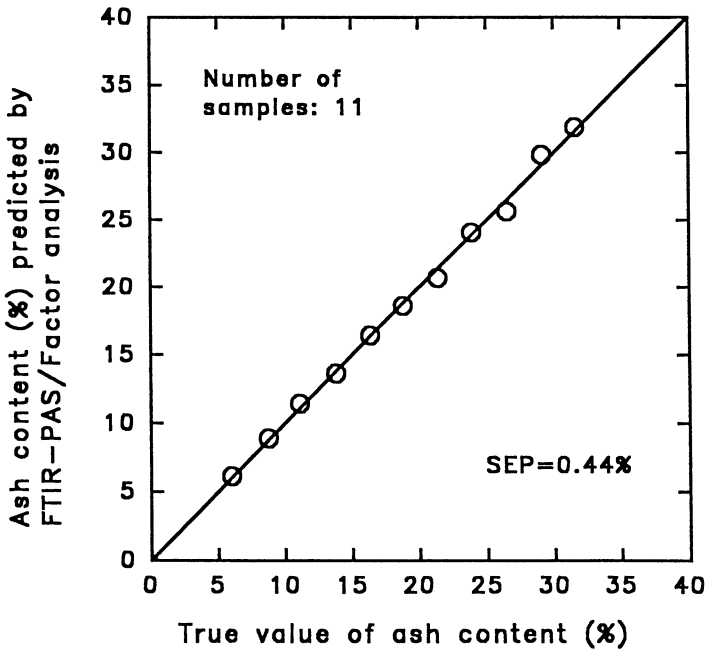

Fig. 24. Cross-correlational plot of ash concentration determined by ASTM ash analysis against predicted concentration determined by FTIR-PAS/factor analysis of cleaned Illinois #6 coal.

D. Variation of Sampling Depth

In Section II signal generation considerations related to sampling depth variation were discussed and an approximate expression for the sampling depth of FTIR-PAS measurements was introduced. In this section, examples are presented where spectra are acquired with different sampling depths by varying FTIR mirror velocity. The first example deals with a homogeneous sample of polycarbonate in order to show that some spectral changes which occur with varying sampling depth are due solely to changes in the degree of absorbance band truncation that appears when the sampling depth is changed. The other examples deal with samples which do have varying compositions with depth.

1. Homogeneous polycarbonate

The top and bottom polycarbonate spectra of Fig. 25 are measured at shallow- and deep-sampling depths, respectively. The top spectrum is reduced so that the heights of the starred small absorbance band just above 2200 cm^{-1} are equal in both the top and the bottom spectra. This band is so weak that it is expected to have little, if any, truncation in either spectrum and consequently is a good feature to use in establishing a consistent scale for these two spectra. After this scaling, it is easy to observe the very significant truncation of strong bands that occurs in FTIR-PAS spectra measured with deep sampling.

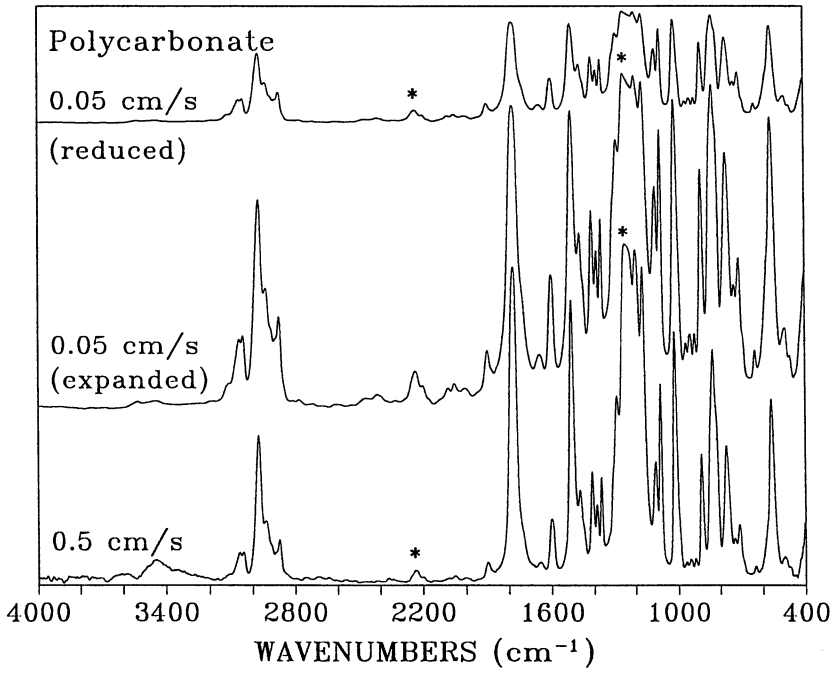

Fig. 25. FTIR-PAS spectra of polycarbonate measured at OPD mirror velocities of 0.05 cm/s (deep-sampling depth) and 0.5 cm/s (shallow-sampling depth).

The middle spectrum of Fig. 25 is expanded so that the strongest band denoted by the star just above 1200 cm^{-1} has the same height as this band in the bottom spectrum. Many of the absorbance band heights in the middle spectrum are now observed to exceed those in the bottom spectrum as, for example, the band at 1600 cm^{-1}. This observation should not, however, be interpreted as an increase in species concentrations with depth. It is instead due to inappropriate scaling, for comparative purposes, of one spectrum relative to the other.

2. Mylar-coated polycarbonate

The next example is a sample with a depth-varying composition consisting of a 2.5 micrometer thick coating of mylar on a polycarbonate substrate. The three top spectra of Fig. 26 show that as sampling depth is increased, more and more of the substrate spectra appear. As the FTIR mirror velocity is decreased from 1.5 cm/s to 0.5 cm/s and finally to 0.05 cm/s, the polycarbonate band at 1775 cm^{-1} is seen to grow relative to the mylar band at 1725 cm^{-1}. Wherever there are bands of little or no spectral overlap, similar behavior is observed allowing differentiation between a number of substrate and coating features.

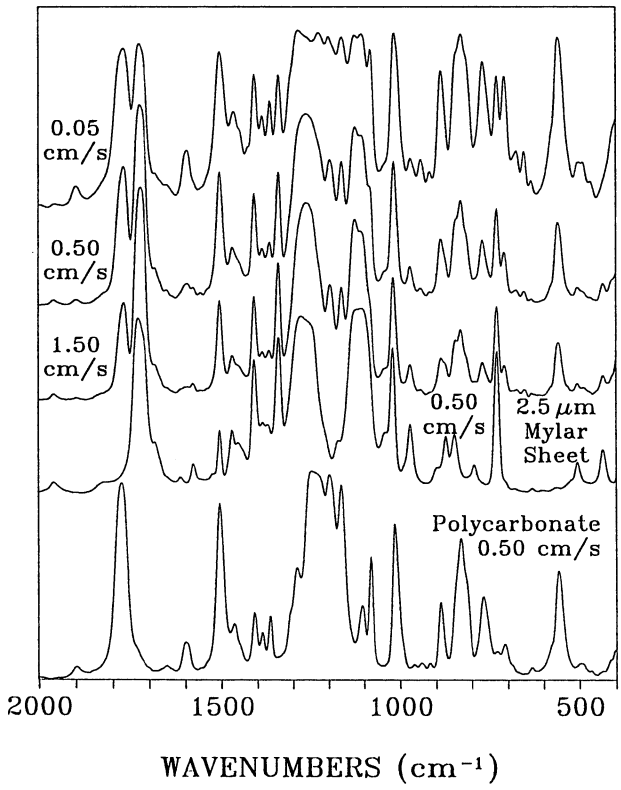

Fig. 26. FTIR-PAS spectra of a 2.5 μm mylar coating on a polycarbonate substrate measured with increasingly deep-sampling depths going from mirror velocities of 1.50, 0.50, and 0.05 cm/s. Spectra of the mylar sheet and polycarbonate alone are shown for comparison with the upper spectra. Note the increasing prominence of the polycarbonate substrate band at 1775 cm^{-1} as the sampling depth increases.

3. Cure of an acrylic coating

The sampling depth variability of FTIR-PAS measurements is especially useful in analysis of coatings where it is desirable to enhance the coating spectrum relative to the substrate spectrum. A typical example is monitoring of cure due to ultraviolet-induced polymerization of an acrylic coating on polycarbonate. The spectra of Fig. 27 show the cure monitoring as indicated by reduction of the cure band height with increasing polymerization. All of the spectra in Fig. 27 are scaled so that the polycarbonate peak heights at 1600 cm^{-1} are equal. Considerably more contrast is observed in the cure bands measured by shallow-sampling than by deep-sampling. Consequently, the more coating-specific shallow-sampling FTIR-PAS analysis provides the most sensitive monitor of the degree of coating cure.

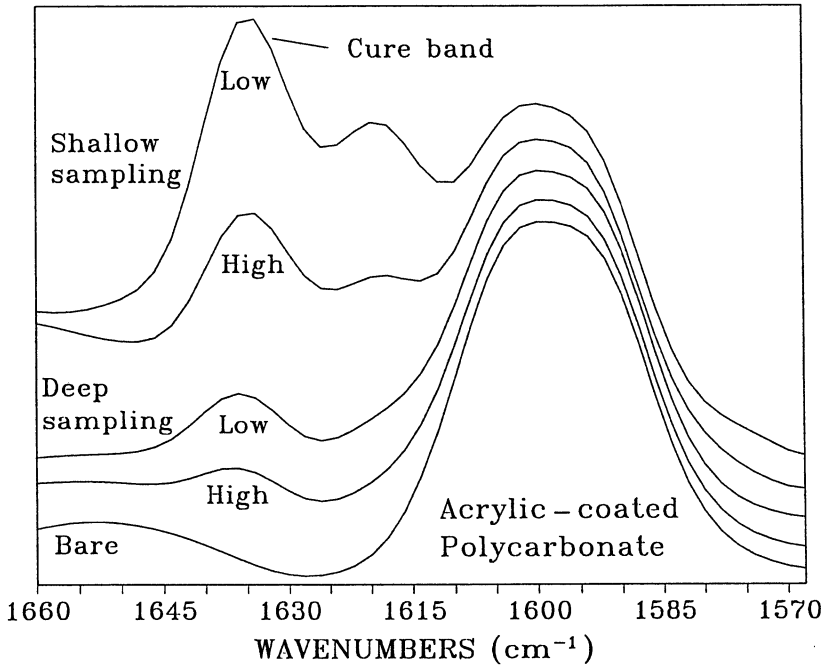

Fig. 27. FTIR-PAS spectra of an acrylic coated polycarbonate with high and low degrees of cure that are measured with shallow and deep sampling. The intensity of the cure band decreases going from a low to a high degree of cure. Note that shallow sampling is most sensitive to the cure process because it enhances the coating versus the substrate spectrum. All spectra are scaled so that the substrate band at 1600 cm^{-1} are of equal height.

4. Plastic-coated paper

Plastic-coated paper is another example of a layered material. The material used in this example has a 35 micrometer thick coating and was analyzed by both FTIR-PAS and DRIFTS in order to probe deeper into this rather thickly coated material than can be achieved by FTIR-PAS alone. A MTEC multisampling option pictured in Fig. 28 was used to measure the DRIFTS spectrum. This option allows DRIFTS, PAS, and transmittance spectra to be obtained rapidly by interchanging sampling heads shown in the foreground of Fig. 28 without changing FTIR accessories.

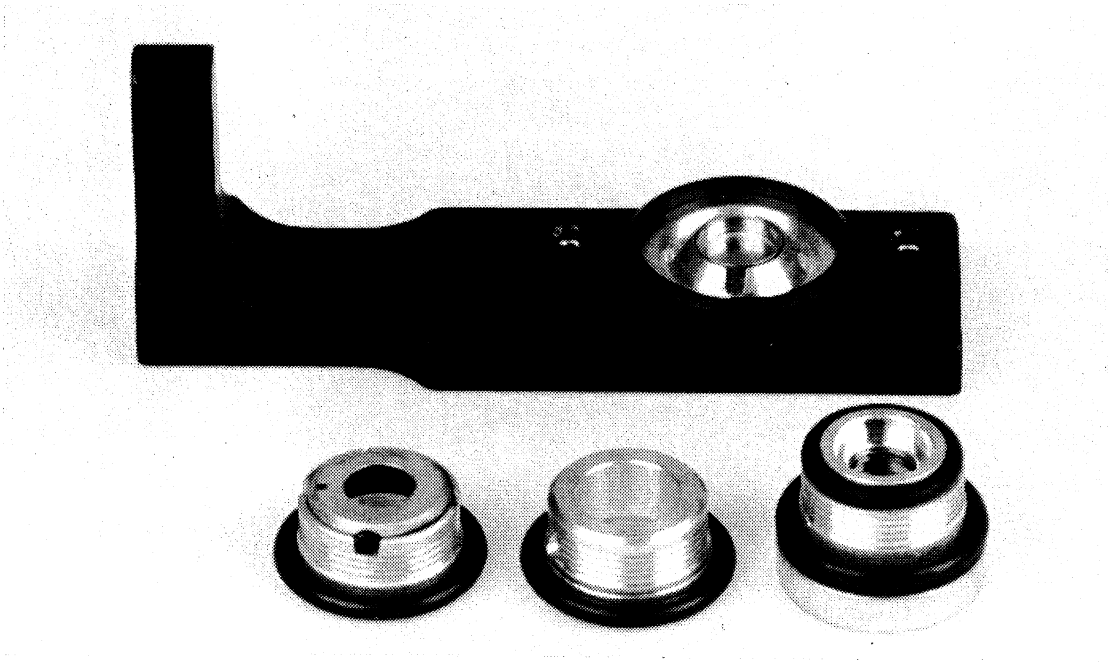

Fig. 28. MTEC multisampling options with interchangeable sampling heads shown in the foreground (left to right) for diffuse reflectance (DRIFTS), photoacoustic (PAS), and transmission sampling. The sampling heads for DRIFTS and transmission operation have carbon black absorber elements incorporated within to sense the fraction of the infrared beam that is diffusely reflected or transmitted, respectively.

Spectra of the paper obtained with shallow- and deep-sampling PAS and DRIFTS are shown in sequence going from bottom to top in Fig. 29. The shallow-sampling photoacoustic spectrum measured at an OPD velocity of 0.5 cm/s is dominated by the absorbance bands of the 35 micrometer thick coating. It is possible in this case to essentially isolate the plastic spectrum by shallow-sampling alone without spectral subtraction due to the coating's thickness and thermal properties.

The deep-sampling spectrum measured at an OPD velocity of 0.05 cm/s reveals additional absorbance bands of the paper such as the feature at 900 cm^{-1}. The DRIFTS spectrum, plotted in Kubelka-Munk units probes still deeper into the paper and shows absorbance bands including the one at 3700 cm^{-1} that are not observed in the photoacoustic spectra. The DRIFTS spectrum also contains artifacts as, for instance, the dip at approximately 1260 cm^{-1}. This feature is due to absorbance by the plastic coating and should be a peak rather than a dip. In spite of some artifacts, the information in the DRIFTS spectrum gives spectral information from deeper within the sample than FTIR-PAS probes at a mirror velocity of 0.05 cm/s. New step-scan FTIR interferometers provide considerably lower mirror velocities which will extend FTIR-PAS sampling depth by over a factor of 3. This advance will yield sampling depths comparable to or greater than DRIFTS on many classes of samples.

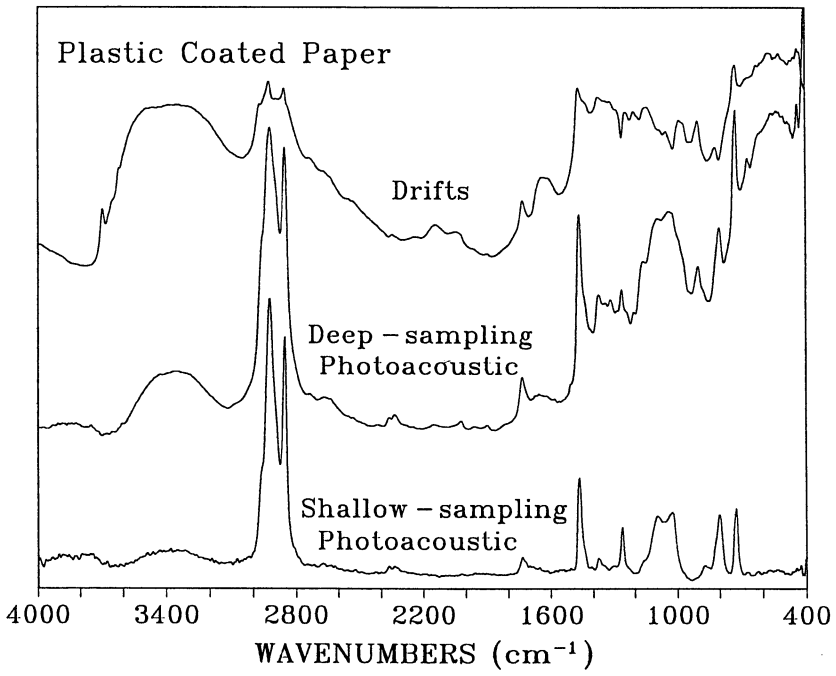

Fig. 29. FTIR spectra of a plastic-coated spectra measured by PAS and DRIFTS sampling. The sampling depth of the spectra increases from the bottom to the top of the figure.

5. Chemically treated surfaces of polystyrene

A final example in this topic deals with infrared analysis of chemically-altered surfaces of polystyrene spheres which are approximately 0.5 mm in diameter. Both FTIR-PAS and DRIFTS spectra are plotted in Fig. 30. The DRIFTS spectrum shows very expanded weak absorbance bands, inverted or derivatized strong bands, and some absent bands. The FTIR-PAS spectra measured at an OPD mirror velocity of 0.5 cm/s show both polystyrene bands and bands due to the chemical treatment. In this instance, it was not possible to isolate the chemically-treated layer from the underlying polystyrene. Consequently, spectral subtraction using a spectrum of untreated polystyrene was necessary in order to isolate the absorbance bands due to the chemical treatment.

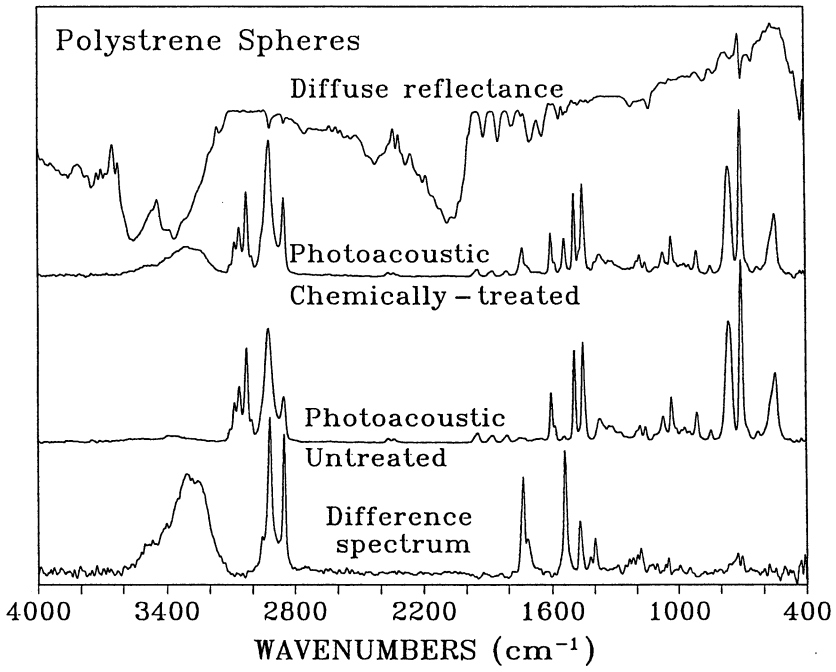

Fig. 30. FTIR spectra of polystyrene spheres with and without chemically-treated surfaces. In this case, the very deep-sampling depth of DRIFTS results in grossly distorted spectra. FTIR-PAS allows the spectrum due to the chemical surface treatment to be observed after spectral subtraction. The samples were provided by Prof. R.A. Kellner of the Institute of Analytical Chemistry, Technical University of Vienna.

E. Carbon-Filled Materials

Materials with significant concentrations of carbon in fiber or powder form are highly opaque and consequently are difficult to analyze by infrared spectroscopy. These materials, however, are of considerable industrial importance and their infrared spectra provide very useful information for research and development and for production operations.

Baseline slope is often present in spectra of very strongly absorbing samples. It is magnified by the need to expand the ordinate scale of spectra to a high degree in order to see absorbance bands above a strong background absorption due, for instance, to carbon black.

There are two basic mechanisms that lead to baseline slope with strongly absorbing samples. The first is due to light scattering within the sample and causes the baseline to slope upwards with increasing wavenumber. The second is due to differences in thermal response as a function of infrared beam modulation frequency between the sample and the reference standard used to ratio spectra. For instance, there is usually less baseline slope with a solid slab sample geometry if the reference standard has the same geometry. Consequently, a slab of glassy carbon or graphite is a preferable reference standard to carbon black in either a thin coating or powder form if a slab of material is being analyzed.

1. Composite material prepreg

Carbon fiber/epoxy prepregs are too opaque for transmission spectroscopy but yield a good FTIR-PAS spectrum of the epoxy component as is shown in Fig. 31. This spectrum was obtained on a 7 mm x 7 mm square of material cut with scissors. The plot shows a baseline that slopes upward with increasing wavenumber which is characteristic of light scattering within the sample.

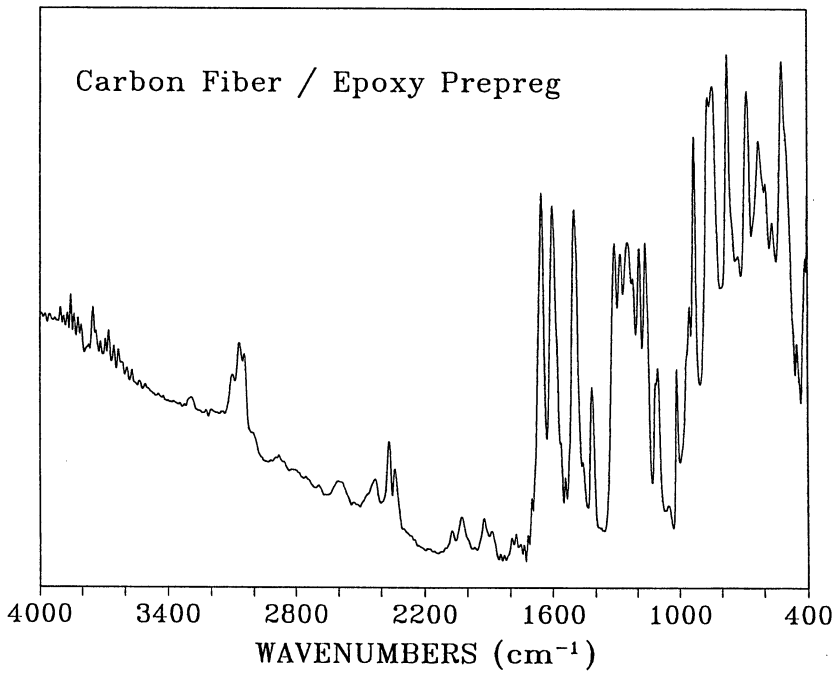

Fig. 31. FTIR-PAS spectrum of a carbon fiber/epoxy prepreg used in composite materials. The spectrum has a sloping baseline due to light scattering within the sample. Absorbance bands appear in the spectrum between 1400 - 1900 cm^{-1} and 3500 - 3900 cm^{-1} due to moisture in the sample chamber. If more time is allowed for purging and for desiccant to work, these bands would be eliminated.

2. Automobile tire

Figure 32 shows a FTIR-PAS spectrum of a typical automobile tire with a high carbon black concentration. Tire samples are among the most difficult materials from which to obtain infrared spectra. The spectrum of Fig. 32 was obtained on a slab of tire cut out with a razor blade. Twenty-thousand FTIR scans were co-added for sample and reference spectra at an OPD mirror velocity of 0.5 cm/s and 8 cm^{-1} resolution.

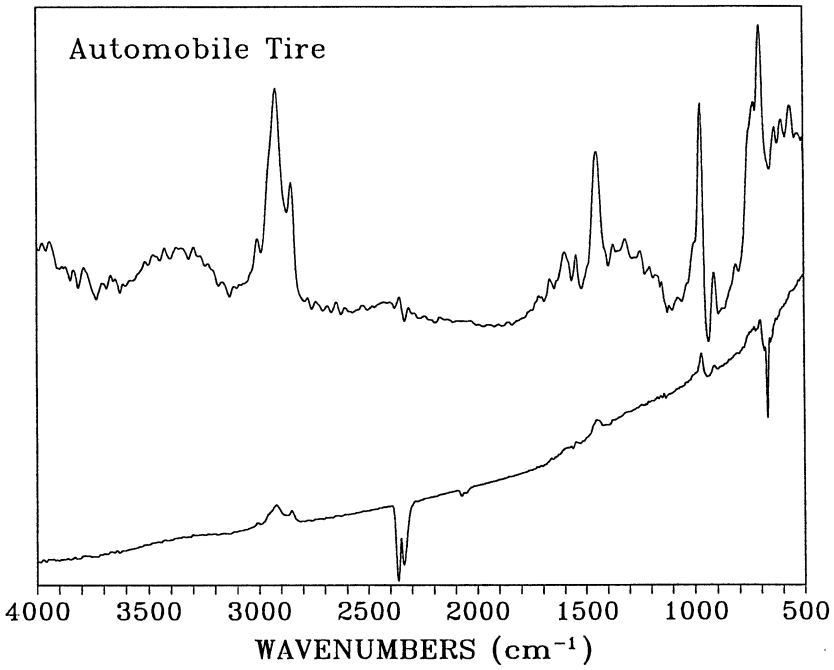

Fig. 32. FTIR-PAS spectra of an automobile tire. The lower spectrum is the ratio of a single beam tire spectrum to a single beam glassy carbon spectrum. The upper spectrum is the result of baseline flattening, subtraction of CO_2 bands and blanking of another gas feature between 2000 and 2100 cm^{-1}, and a 19 point smoothing.

F. Polymer Films

1. Elimination of interference fringes by FTIR-PAS

Interference fringe bands are often observed in infrared transmission spectra of polymer films. These bands interfere with and obscure important small features in spectra associated with various types of additives. FTIR-PAS spectra are free of interference artifacts due to the differences in signal generation between an absorption versus transmission based measurement.

Figure 33 shows spectra measured by the conventional transmission method and by FTIR-PAS of the same polyethylene film. The spectra were measured directly on the film material after punching out a disk of the film with a cork borer. The FTIR-PAS spectrum

has been plotted as a transmission spectrum using the procedure discussed in Section V.A.1. Many of the small- and medium-sized features of the conventional transmission spectrum are so seriously distorted that they are not discernable for a qualitative analysis and that observable features are not useful for quantitative analyses. For instance, it is not possible to observe the small band at 2330 cm^{-1} in the transmission spectrum and the larger band at 1100 cm^{-1} is not suitable for quantitative analysis due to the fringe bands.

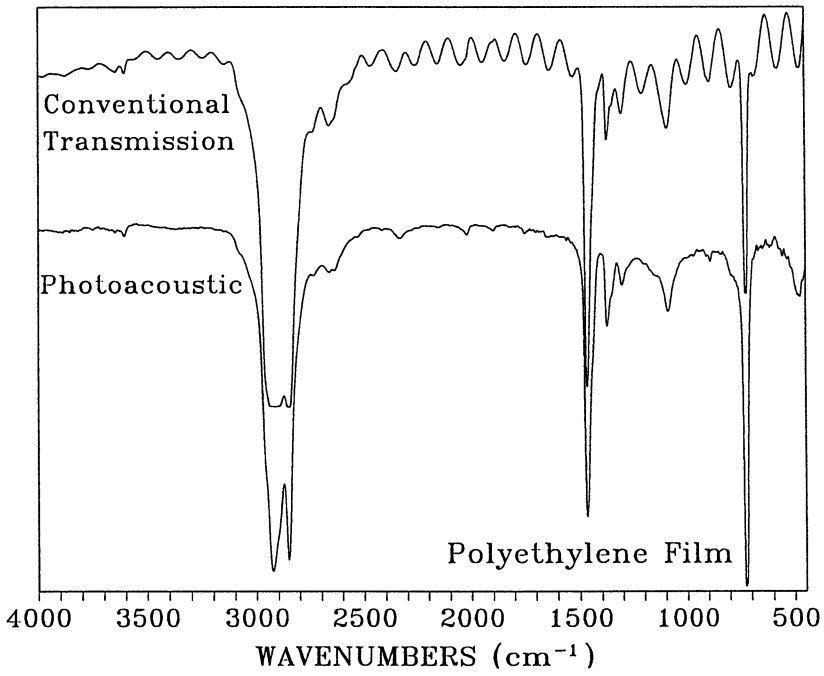

Fig. 33. Conventional transmission and FTIR-PAS spectra of a 32 micrometer thick polyethylene film. The PAS spectrum has been converted to transmittance for the purpose of comparison. Note the absence of interference fringes in the PAS spectrum.

2. Polarized beam measurements on oriented films

In production, polymer fibers are oriented by drawing in order to improve tensile strength. Polarized FTIR-PAS measurements are useful in monitoring the orientation process. A polarizer is placed in front of the photoacoustic detector so that the infrared beam incident on the sample in the detector's sample holder is polarized. It may be useful to initially rotate the polarizer until the signal is maximized with a carbon black reference in the detector. This procedure will ensure that the polarizations imposed by the FTIR optics and the polarizer are in coincidence resulting in maximal intensity in the polarized beam.

After this adjustment, the polarizer should be left fixed and the sample should be rotated in the sample cup. Figure 34 shows spectra of a PET film with the infrared beam polarized parallel and perpendicular to the direction of draw. A number of spectral changes are observed as a function of orientation particularly in the 800 - 900 cm^{-1} and 1300 - 1400 cm^{-1} ranges. The absence of interference fringes in FTIR-PAS spectra is obviously also an advantage in this application.

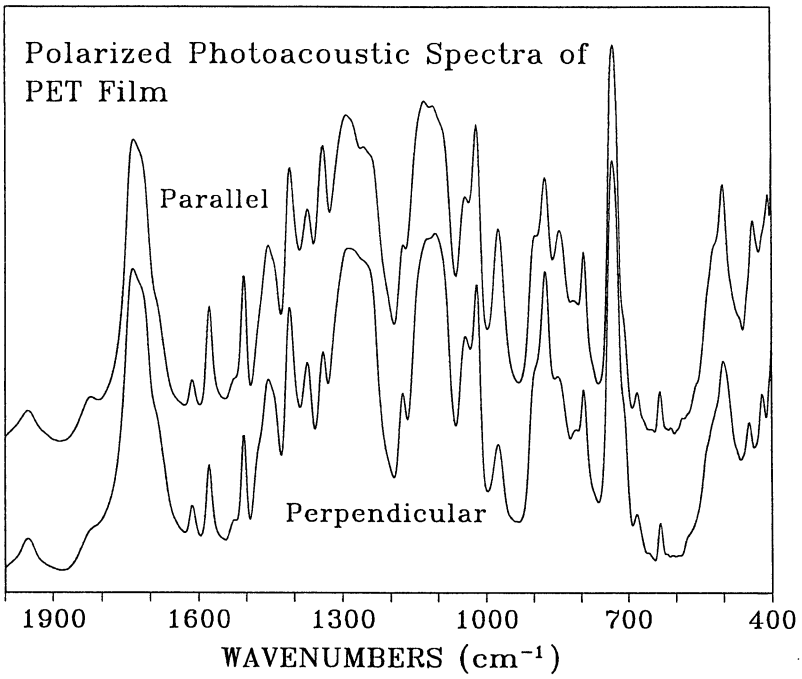

Fig. 34. FTIR-PAS polarized light spectra of a 31 micrometer thick PET film which has been drawn in production to induce molecular orientation. Spectra were measured with the direction of draw oriented parallel and perpendicular to the polarization direction of the infrared beam.

3. Polymer coatings on metal containers

Polymer films are often used as a barrier coating on beverage and food containers. Figure 35 shows a FTIR-PAS spectrum of a polymer coating on the interior of a beverage can. The spectrum was measured directly on a small specimen cut with scissors from the can. The surface morphology of such a specimen is of no consequence in a FTIR-PAS measurement whereas surface flatness is critical in a specular reflectance measurement that the reflected fraction must be focused on the detector.

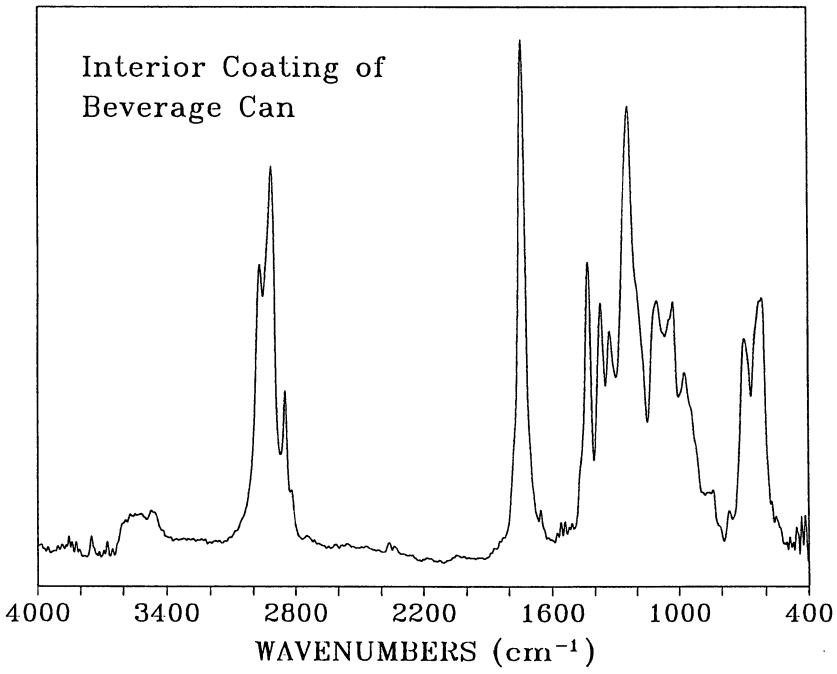

Fig. 35. Infrared spectrum of a beverage can's internal coating measured by FTIR-PAS.

G. Semisolids, Gels, and Liquids

FTIR-PAS can be applied to semisolid, gel, and liquid samples when considerations of light scattering or contact with infrared window materials makes transmission or ATR methods impractical. In these instances only enough sample should be used to cover roughly a 5 mm diameter area centered in a stainless steel cup or other vessel. If the sample is aqueous a desiccant should be used under the sample cup as discussed in Section III.A. Lower mirror velocities will help in reducing the intensity of vapor spectra which may be superimposed on the sample spectrum. If necessary, spectral subtraction can be used to remove the vapor spectrum. A spectrum of the vapor alone can be obtained by covering the sample with a small disk of aluminum foil and thereby masking the sample from the infrared beam. The vapor will still be present above the foil and will produce only a vapor spectrum.

Figure 36 shows a spectrum of an aqueous collagen gel which is primarily water obtained with a desiccant but without spectral subtraction to remove the small amount of moisture and CO_2 spectra that are present. The spectrum clearly shows the absorbance bands of the non-water species.

Care should be taken when vapor species are associated with samples to avoid vapors that might damage or contaminate the photoacoustic detector.

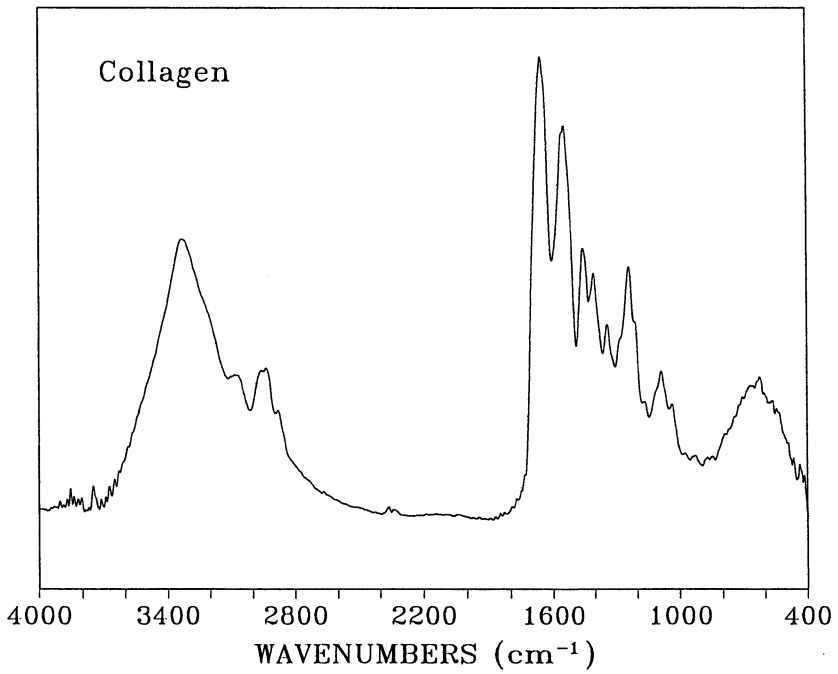

Fig. 36. FTIR-PAS spectrum of an aqueous collagen gel.

VI. CONCLUSION

PAS provides the FTIR spectroscopist with a rapid non-destructive means of directly obtaining spectra of materials without traditional sample preparation to reduce opacity. The PAS method is applicable to all types of samples in macro and micro forms. FTIR-PAS spectra have the same absorbance peak wavenumber locations as classic transmission spectra but usually have truncation of strong absorbance bands due to photoacoustic signal saturation. The presence of band truncation, however, has not been found in applications explored to date, to limit the capability of FTIR-PAS in either qualitative or quantitative determinations based on commercial FTIR search and factor analysis software, respectively.

FTIR-PAS has the unique capability of being able to vary sampling depth by changing the modulation frequency of the FTIR beam. This capability allows, for instance, measurement of spectra with either high surface specificity to analyze a coating, or with bulk specificity to observe the absorbance bands of a substrate.

Other important aspects of FTIR-PAS measurements include operation over all spectral regions, absence of interference fringes, elimination of microsample pressing and aperturing, and capability to switch between sampling modes by interchanging photoacoustic detector sampling heads for DRIFTS, PAS, and transmission analyses.

VII. ACKNOWLEDGEMENTS

This work was funded by MTEC Photoacoustics, Inc.; by the Center for Advanced Technology Development, which is operated by Iowa State University for the U.S. Department of Commerce under Grant No. ITA 87-02; and by Ames Laboratory, which is operated by Iowa State University for the U.S. Department of Energy under Contract No. W-7405-ENG-82, and supported by the Assistant Secretary for Fossil Energy.

We wish to thank the following people for supplying samples used in this work: J.B. Callis (Univ. of Washington), L. Bright (DuPont), H.L.C. Meuzelaar (Univ. of Utah), M.W. Tungol and E.G. Bartick (FBI), P. Milne (Univ. of Miami), P.J. Codella (General Electric), B.J. Slomka and W.H. Buttermore (Ames Laboratory) and R. Kellner (Technical University of Vienna).

VIII. REFERENCES

1. Colthup, N.B.;Daly, L.H.; Wiberley, S.E. Introduction to Infrared and Raman Spectroscopy; 3rd ed., Academic: New York, 1990.

2. Laboratory Methods in Infrared Spectroscopy; 2nd ed., R.G.J. Miller and B.C. Stace, Eds.; Heyden and Sons: London, 1979.

3. Practical FTIR Spectroscopy: Industrial and Laboratory Chemical Analysis; J.R. Ferraro and K. Krishnan, Eds.; Academic: New York, 1990.

4. Osborne, B.G.; Fearn, T.; Near Infrared Spectroscopy in Food Analysis; Longman Scientific and Technical: Essex, UK, 1986.

5. Graham, J.A.; Grim, W.M., III; Fateley, W.G.; Fourier Transform Infrared Photoacoustic Spectroscopy of Condensed-Phase Samples, in Fourier Transform Infrared Spectroscopy, Vol. 4; J.R. Ferraro, L.J. Basile, Eds.; Academic: Orlando, 1985.

6. Griffiths, P.R.; de Haseth, J.A.; Fourier Transform Infrared Spectrometry; Wiley: New York, 1986, p. 45.

7. Crocombe, R.A.; Compton, S.V.; The Design, Performance and Applications of a Dynamically-Aligned Step-Scan Interferometer, FTS/IR Notes No. 82; Bio-Rad, Digilab Division, Cambridge USA, 1991.

8. Michaelian, K.H. Appl. Spectrosc. **1989**, 43, 185.

9. McDonald, F.A. Am. J. Phys. **1980**, 48, 41.

10. Carslaw, H.S.; Jaeger, J.C.; Conduction of Heat in Solids; Clarendon: Oxford, 1959.

11. Dittmar, R.M.; Chao, J.L.; Palmer, R.A. Appl. Spectrosc. **1991**, 45, 1104.

12. Oelichmann, J. Freseuius Z. Anal. Chem. **1989**, 333, 353.

13. Kinsler, L.E.; Frey, A.R.; Fundamentals of Acoustics, 2nd ed., Wiley: New York, 1950; p. 186.

14. Griffiths, P.R.; de Haseth, J.A.; Fourier Transform Infrared Spectrometry; Wiley: New York, 1986.

15. Perkin-Elmer Polymer Library; D.O. Hummel; Perkin-Elmer: Norwalk.

16. Tungol, M.W.; Bartick, E.G.; Montaser, A. Appl. Spectrosc. **1990**, 44, 543.

17. McCrone, W.C.; Delly, J.G.; The Particle Atlas: An Encyclopedia of Techniques for Small Particle Identification, 2nd ed.; Ann Arbor Science: Ann Arbor, 1973-1980.

18. Haaland, D.M.; Thomas E.V. Anal. Chem. **1988**, 60, 1202.

19. Haaland, D.M.; Thomas E.V. Anal. Chem. **1988**, 60, 1193.

20. Malinowski, E.R.; Hovery, D.G. Factor Analysis in Chemistry; Wiley, New York, 1980.